Antarctic Science 9 (1): 74–91 (1997)

A revised Archaean chronology for the Napier Complex, Enderby Land, from SHRIMP ion-microprobe studies

S.L. HARLEY[1] and L.P. BLACK[2]

[1]*Department of Geology and Geophysics, Grant Institute, University of Edinburgh, West Mains Road, Edinburgh EH9 3JW, UK*
[2]*Division of Regional Geology and Minerals, Australian Geological Survey Organisation, GPO Box 378, Canberra, ACT 26001, Australia*

Abstract: The long and complex Archaean evolution of the Napier Complex of Enderby Land, characterized by high-grade metamorphism and several strong deformations, is reassessed in the light of new SHRIMP U–Pb zircon dating results bearing on the ages of protoliths and possible regional extents of distinct Archaean tectonothermal events. Initial felsic igneous activity occurred over a significant time interval *c.* 3800 Ma ago. An age of 2980±9 Ma for the emplacement of charnockite at Proclamation Island might date the oldest tectonothermal event to be recognized in the Napier Complex. An ensuing, very-high grade, previously imprecisely dated tectonothermal event occurred at 2837±15 Ma. U–Pb zircon ages ranging from 2456+8/-5 Ma to 2481±4 Ma date a subsequent, protracted high-grade tectonothermal event. Whereas the ~2840 Ma event is of regional importance in the Amundsen Bay-Casey Bay area, it is possible that the ~2980 Ma event was of only moderate grade, minor importance, or even absent, in that part of the Complex. If so, the apparent trend to very-high temperature metamorphism in the Tula and Scott mountains compared with the Napier Mountains may reflect two distinct metamorphic events rather than a simple baric and thermal gradient. The oldest crustal component in the Napier Complex appears to have been of igneous derivation. Zircon populations in paragneisses at Mount Sones are similar to those in the nearby orthogneisses, which therefore may have been basement. Another paragneiss, in the Casey Bay area, yields no zircons older than 2840 Ma, probably indicating that pre-3000 Ma crust, which is now located nearby, was not exposed at the time of sedimentation there. The isotopic data are quite complex, particularly in rocks that experienced post-crystallization metamorphic temperatures of 1000°C or more. It is postulated that this complexity, which was largely the product of migration of radiogenic Pb within the zircon grains in ancient times, and produced local excesses of this element with respect to its parent U, was caused by volume diffusion at these abnormally high regional crustal temperatures.

Received 5 September 1996, accepted 3 October 1996

Key words: Antarctica, granulite, Napier Complex, SHRIMP, zircon

Introduction

The Napier Complex of Enderby Land (Ravich & Kamenev 1975) (Fig. 1) is one of several known Archaean blocks within the East Antarctic Precambrian Shield (Black *et al.* 1992). The complex has attracted a great deal of geological interest because of its great antiquity, and the very high-grade and multiply-deformed nature of its rocks, which include both orthogneisses and a variety of paragneisses. Ultra-high temperature (UHT) granulite-facies mineral assemblages such as sapphirine and quartz, orthopyroxene and sillimanite, and osumilite (Dallwitz 1968, Sheraton *et al.* 1980, 1987, Ellis *et al.* 1980, Grew 1980) indicate peak metamorphic conditions of *c.* 950–1030°C and 0.7–1.1 GPa (Ellis *et al.* 1980, Ellis 1980, 1983, Harley 1983, 1985, 1987, Harley & Black 1987) at about the time of the first recognized deformation (D_1 of James & Black 1981, Black & James 1983).

Reports of Pb–Pb ages of *c.* 4000 Ma for orthogneisses from the Fyfe Hills (Ravich *et al.* 1975, Sobotovich *et al.* 1976) generated intense interest in the age of the Napier Complex, and appeared to be supported by initial ion-microprobe studies (Lovering 1979, 1980). SHRIMP U–Pb zircon analyses (Black *et al.* 1986a) produced a similar age of 3927±10 Ma for orthogneiss from Mount Sones, but Rb–Sr and conventional U–Pb zircon studies (Black *et al.* 1986b) showed that felsic magmatism also occurred at considerably younger times. As a result, the major objectives of previous isotopic dating has been to discover the ages of the orthogneiss protoliths and to date the three major tectonothermal events defined by Sheraton *et al.* (1980) and Black & James (1983). This has proven to be a difficult task because the high grade and complex history has led to partial (or even total) resetting of isotopic systems (e.g. K–Ar, Rb–Sr, Sm–Nd and U–Pb zircon: Krylov 1972, Black *et al.* 1983a, Black & McCulloch 1987, Williams *et al.* 1984). Indeed, the strong isotopic imprint of an important granulite facies event at or near 2500 Ma (James & Black 1981, Black & James 1983, Grew *et al.* 1982, Black *et al.* 1983b) has obscured much of the earlier history.

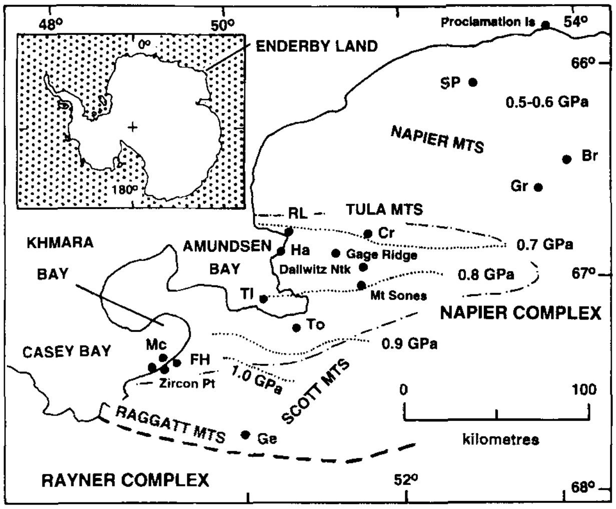

Fig. 1. Outcrop map of Enderby Land showing sample locations and key geological features noted in the text. Dotted lines = isobars defined by a combination of geobarometry and phase equilibria (Harley 1983, 1985, 1987), with pressures in GPa (modified after Harley & Hensen 1990). Dot-dashed line = approximate limits of ultra-high temperature assemblages sapphirine + quartz and orthopyroxene + sillimanite + quartz. Abbreviations for localities as follows:
Br = Mount Bride; Cr = Crosby Nunataks; FH = Fyfe Hills; Ge = Mount George; Gr = Grimsley Peaks; Ha = Mount Hardy; Mc = McIntyre Island; RL = Mount Riiser Larsen; SP = Simmers Peaks; TI = Tonagh Island; To = Mount Tod.

A combination of Rb–Sr, Sm–Nd and zircon U–Pb geochronology was applied by Black *et al.* (1986b) and Sheraton *et al.* (1987) to the most precisely dated samples that could be assigned to critical parts of the tectonothermal history. These studies defined a polyphase deformational and metamorphic history with D_1–M_1, D_2–M_2 and D_3–M_3 proceeding at 3070±34 Ma, *c.* 2900 Ma and 2456+8/-5 Ma, respectively. This history is summarized in Table 1 for comparison with the chronology developed here. Only the age defined for D_3–M_3 is both precise and derived from the relatively resistant U–Pb zircon system. Hence, there remains some doubt about the geological significance of the old ages assigned to D_1–M_1 and D_2–M_2, which are considered by some workers to have also occurred at *c.* 2500 Ma (Grew & Manton 1979, Grew *et al.* 1982, DePaolo *et al.* 1982, Sandiford & Wilson 1984).

SHRIMP ion-microprobe dating is clearly a key technique for dating discrete events in a terrain as complicated as the Napier Complex. Yet, until now, only one rock from this terrain has been dated using this approach (Black *et al.* 1986a). SHRIMP data for six new rocks and for a previously analysed orthogneiss sample at Mount Sones are used here in an attempt to resolve some of the current uncertainties in the chronostratigraphy of the Napier Complex and develop a revised model for the crustal evolution of this Archaean high-grade terrain.

Analytical methods

Zircons were extracted from the disaggregated rock samples using standard heavy liquid and magnetic separation techniques and mounted in epoxy discs which were polished and gold-coated prior to ion microprobe analysis. Small fragments of a standard zircon were mounted directly with the samples to minimize any erratic inter-element fractionation that sometimes arises because of slight differences in the surface alignments when separate standard plugs are used. U–Pb analyses were carried out using the SHRIMP II ion microprobe at the Australian National University, Canberra, following the standard techniques described by Compston *et al.* (1984) and Williams *et al.* (1984). Pb/U and Pb/Pb isotopic ratios were measured at a mass resolution of 6500. Pb/U ratios were corrected for instrumental mass fractionation using ratios measured on the standard zircon SL13($^{206}Pb/^{238}U$ = 0.0928) combined with a power-law calibration curve relating Pb+/U+ to UO+/O+. Common Pb corrections were negligible for all samples (< 1% ^{206}Pb), and were based on the measured ^{204}Pb. The assumed common Pb composition was modelled as contemporaneous Pb (Cumming & Richards 1975) in all cases. All data, including mean ages derived from linear regressions of zircon populations, are reported with 2-σ uncertainties. Analytical data are plotted in the concordia diagrams as 2-σ error polyhedra.

Interpretation of isotopic data, and implications for the cause of radiogenic Pb loss

It is important to address here the rationale behind the interpretation of the data from the various samples. In general the data form complex arrays, largely due to an effect that has been documented by the only previous SHRIMP study of this terrain (Williams *et al.* 1984, Black *et al.* 1986a), namely the movement of radiogenic Pb within the zircon lattice in ancient times. Although this phenomenon might have occurred to limited extents elsewhere, there are at present no other accounts of it being so pronounced. Its strong development in the Napier Complex must relate to the geological uniqueness of this region (see below). Normally $^{207}Pb/^{206}Pb$ ages can be reliably interpreted as minimum ages for zircon growth but, as Williams *et al.* (1984) have shown, ancient Pb migration leads to $^{207}Pb/^{206}Pb$ ages that can overestimate, underestimate, or even be realistic estimates of zircon crystallization. A logical approach to this problem (Williams *et al.* 1984) is to regress related analyses on a conventional $^{207}Pb/^{235}U$–$^{206}Pb/^{238}U$ concordia diagram, and assign the upper concordia intercept age to the time of zircon growth. However, it is not always possible to ascertain with certainty whether or not particular analyses can be justifiably included on such a regression. In an effort to resolve this uncertainty, we have also plotted the analyses on probability

https://doi.org/10.1017/S0954102097000102 Published online by Cambridge University Press

Table I. Summary and comparison of Napier Complex history.

Age/time interval (Ma)	Event(s) (This work)	Age/time interval (Ma)	Event(s) (Sheraton *et al.* 1987)
3840–3770	Crystallization of igneous precursors to older orthogneisses (Tula Mountains).	3950–3800	Mount Sones orthogneiss precursors emplaced. Early crust in Fyfe Hills.
pre-2980	Deposition of supracrustal sequences sourced by older orthogneisses.	pre-3070	Deposition of supracrustal sequences.
2980	Crystallization of Proclamation Island charnockite. D_1(P) deformation and metamorphism. Granulite facies metamorphism at >800°C and 0.5–0.8 GPa in Napier Mountains and possibly other parts of the complex.	3100–3000	Syn-D_1 (M1) emplacement of Proclamation Island charnockite. Isoclinal folding, intense fabrics over the whole Napier Complex. Very-high temperature metamorphism at 900–1000°C and 0.7–1.1 Gpa. Possible prograde replacement of cordierite by sapphirine + quartz (Motoyoshi & Hensen 1989).
2980–2840	Exhumation of Napier crust, deposition of supracrustal sequences.	3000–2900	D_1 to D_2 interval: gneisses remain under deep-crustal conditions.
2840–2820	Deformation and metamorphism of older crust and new supracrustals under ultra-high temperature conditions in Tula and Scott mountains [D_1–D_2(S and T)]. Intrusion of precursors to young orthogneisses.	2900	Regional D_2 event producing tight and asymmetric folds. Continued granulite facies conditions, variable grade from N to S.
2840	Emplacement of granitoids in Napier Mountains (Mount Bride).	2840	Emplacement of granitoids in Napier Mountains (Mount Bride).
2840–2480	Near isobaric cooling at 0.7–1.0 GPa.	post-2900	Near isobaric cooling at 0.7–1.0 Gpa.
2480–2450	D_3–M_3 tectonothermal events: upright folds lower-temperature granulite and upper amphibolite facies metamorphism.	2450	D_3–M_3 tectonothermal events: upright folding and lower granulite to upper amphibolite facies conditions 650–700°C and 0.5–0.8 Gpa. Pegmatites emplaced (Grew *et al.* 1982).
2410	Late granites (Simmers Peak).	2410	Late granites (Simmers Peak).

distribution diagrams. These sum the gaussian distribution equivalents of each individual analysis and hence are a better portrayal of overall probability than ordinary histograms, which incorporate only the mean values of each analysis. In practice, the probability distribution diagram sums the attendant probability envelopes of individual analyses, thereby giving proportionately more weight to more precise data. The form of the final curve for a sample is obtained by summing all the components of individual analyses at any particular value of the abscissa ($^{207}Pb/^{206}Pb$ age). Because of the nature of the construction, the ordinate has no absolute significance, but only serves to illustrate the relative frequencies of the various age components. We have used the nature of the overall probability distribution trend for each sample to help decide whether there appear to be distinct age populations in the data (these will be significant only if these data are concordant – as determined by their positions on the concordia diagram), in which case these ages are taken as being geologically significant. If there are no obvious concentrations of concordant data, the age is derived by regression, as described above.

In essence, the regression procedure has been followed when there is evidence of marked post-crystallization isotopic resetting. The samples displaying this effect are those from the southwest of the Napier Compex that crystallized before the UHT event (described above), which was so intense in that region. It would therefore appear that processes associated with that event are responsible for the loss of radiogenic Pb from zircon in the Archaean. Perhaps the prevailing temperatures of 1000°C or more were sufficiently high to cause Pb loss by volume diffusion, a phenomenon that has not been demonstrated in other geological terrains. It might well be that the best isotopic evidence of such a process is provided by frequent local excesses of radiogenic Pb (as documented below) that developed as Pb slowly diffused from the zircon lattice. For example, such excesses could have occurred when Pb from an originally high-U part of the zircon was trapped by falling temperatures in a region with lower U before it could escape the crystal. In contrast, leaching of Pb by fluid ingress or recrystallization of the zircon lattice would be a far more efficient processes in removing Pb before local excesses could accumulate.

https://doi.org/10.1017/S0954102097000102 Published online by Cambridge University Press

Analytical results

3770–3840 Ma orthogneisses

Three examples of early Archaean orthogneiss precursors have been identified from Mount Sones and Gage Ridge in the Tula Mountains. All samples contain subhedral to euhedral, magmatic-habit zircons, which are commonly elongated. Grains with rounded metamorphic rims and zoned cores, are also common (Appendix 1).

A new age estimate has been obtained for the massive granodioritic-tonalitic gneiss (78285007) that forms the south-eastern part of Mount Sones (Fig. 1), based on reanalysis of the sample dated by Black *et al.* (1986a), who derived an age of 3927±10 Ma for the volumetrically dominant zoned zircon and interpreted this as the crystallization age of the precursor of the gneiss. The reality of this age was tested here through preferential analysis of the potentially oldest zircon grains, selected on the basis of reconnaissance $^{207}Pb/^{206}Pb$ ratios. Twenty six analyses of eight clear, unzoned, elongate but rounded grains define concordia intercepts of 3800+50/-100 Ma and 2950±350 Ma (Fig. 2a). On the probability distribution diagram (Fig. 2b) the data are broadly spread about a maximum at about the same value as the upper concordia intercept. The precision of the concordia intersept ages is poor because, in common with Black *et al.* (1986a), the data alignment is subparallel to concordia (Fig. 2a). Many of the analyses plot above concordia, a trend that Williams *et al.* (1984) ascribed to the preferential incorporation, through isotopic migration, of radiogenic Pb into these parts of the zircon grains. This migration must have occurred in ancient times, because the data do not project towards the origin. An alternative explanation of reversely discordant SHRIMP data has recently been proposed by Wiedenbeck (1995), who correlated this phenomenon in a ^{204}Pb-rich zircon with $^{204}Pb/^{206}Pb$. He was able to characterize an ancient labile Pb component resident in amorphous domains in zircon, from which the secondary ion yield of Pb was higher than of radiogenic Pb in the typical zircon lattice. This explanation is not applicable for our analyses, which differ in three vital respects from those of Wiedenbeck (1995).

1) The Mount Sones zircons have a pronounced correlation between Pb/U and $^{207}Pb/^{206}Pb$ (Fig. 2).

2) They have dramatically lower common lead contents (compare the $^{206}Pb/^{204}Pb$ values in Table II with the extremely low values (48–56) reported by Wiedenbeck (1995).

3) Unlike the Wiedenbeck (1995) data, the Zr2O+ emission for the Mount Sones zircons was the same as that for interspersed analyses of the standard zircon. The reverse discordance for Mount Sones zircons is therefore caused by ancient Pb loss, and is not an analytical artefact.

Despite its poor precision, our crystallization age of the igneous precursor to the orthogneiss is clearly *c.* 100 Ma

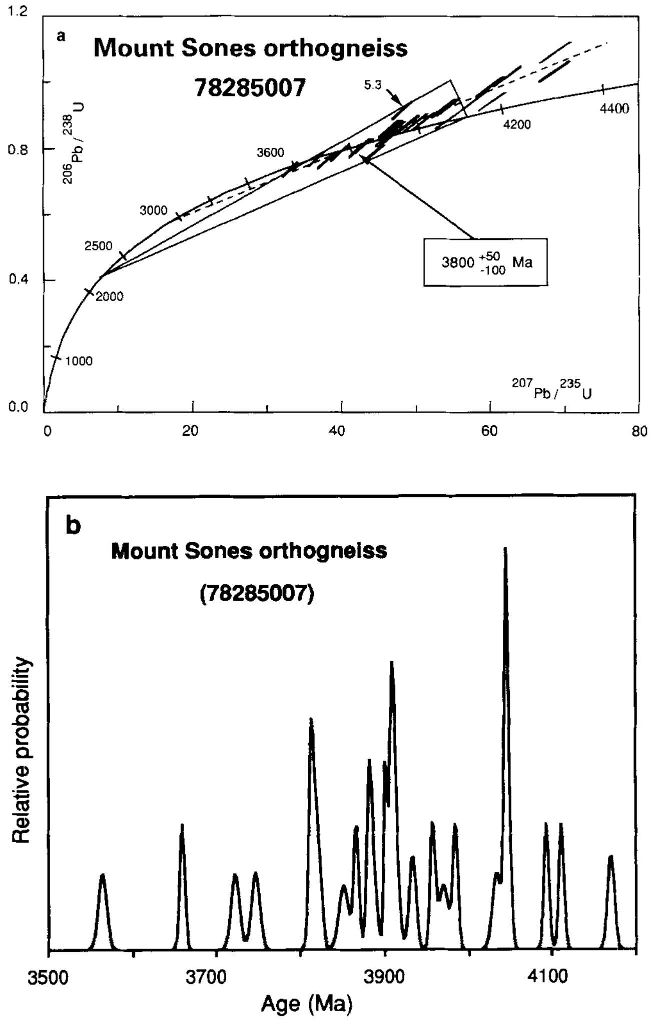

Fig. 2. a. $^{207}Pb/^{235}U–^{206}Pb/^{238}U$ concordia diagram for zircons from orthogneiss (78285007) at Mount Sones. Except for analysis 5.3, all analytical points fit a discordia with an upper intercept at 3800 +50/-100 Ma, which is ascribed to the age of the tonalitic precursor of this gneiss. The shaded triangular field represents the range of earlier analyses obtained for this rock by Black *et al.* (1986a). **b.** Probability distribution diagram for the same sample showing a range of ages broadly centered on the same value as given by the upper concordia intersect.

younger than that obtained by Black *et al.* (1986a). The new age of 3800 Ma is superior to the previous estimate because of the calibrational improvements listed above. We consider that the Pb/U ratios derived by Black *et al.* (1986a) were erroneously low, leading to the upper intercept age being overestimated and the lower intercept age being underestimated. The poor precision of the latter prohibits unambiguous interpretation of its significance.

SHRIMP analyses for a tonalitic orthogneiss (77283465) from better-layered gneisses 6 km NNE of the original Mount Sones sample (Fig. 3a) approximate a straight line (MSWD = 5.5) with concordia intercepts at 3773 + 13/-11 Ma and

https://doi.org/10.1017/S0954102097000102 Published online by Cambridge University Press

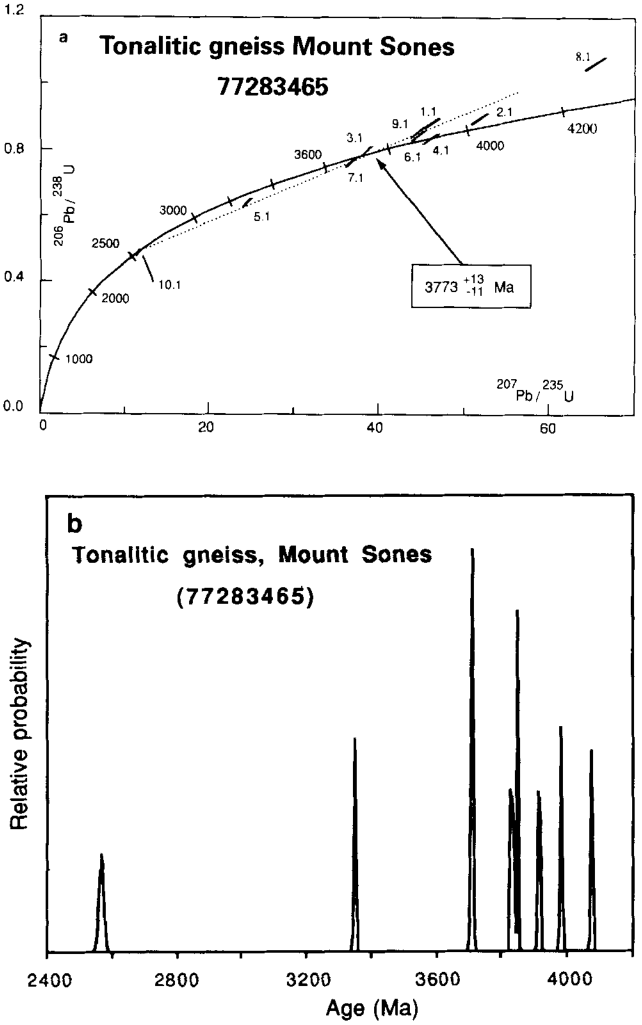

Fig. 3. a. $^{207}Pb/^{235}U$–$^{206}Pb/^{238}U$ concordia diagram for zircons from tonalitic gneiss (77283465) at Mount Sones. A regression through the data has an upper concordia intercept at 3773 +13/-11 Ma, which is believed to be the age of the igneous precursor of this gneiss. **b.** The old analyses on the probability distribution diagram overestimate the age of this event because they are reversely discordant.

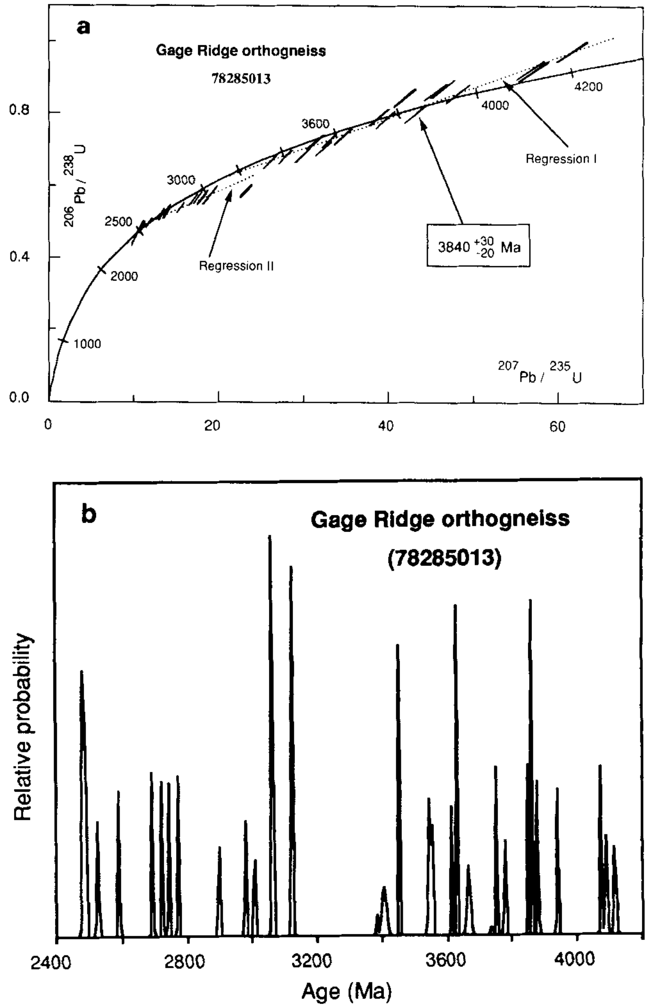

Fig. 4. a. $^{207}Pb/^{235}U$–$^{206}Pb/^{238}U$ concordia diagram for zircons from orthogneiss (78285013) at Gage Ridge. The upper concordia intercept at 3840 +30/-20 Ma for the older analyses defines the age of the igneous precursor of this gneiss. **b.** The probability distribution diagram shows a rather even spread of analyses upwards from the time of the last major event (at *c.* 2450 Ma) to have affected this region.

2600±200 Ma. The older age, derived from cores of elongate prismatic zircon, is believed to be the age of the igneous precursor. This age is indistinguishable from the less precise one obtained from 78285007, and both orthogneisses have similar Sm–Nd isotopic compositions (Black & McCulloch 1987), consistent with them having formed during the same magmatic event. The probability distribution diagram (Fig. 3b) is not nearly as well suited to determine a relatively precise age for these analyses, largely because the bulk of the old analyses are reversely discordant.

A massive granitic orthogneiss (78285013) from Gage Ridge (Fig. 1) contains medium to dark brown, commonly strongly zoned and well rounded zircons. Though some reversely discordant analyses occur (Fig. 4a), most of the zircon data plot below concordia in two isotopic alignments. The older alignment has concordia intercepts of 3840+30/-20 Ma and 3100+220/-270 Ma; the younger alignment intercepts are at 3700+230/-250 Ma and 2590+40/-80 Ma. As there are no consistent morphological or chemical differences between the zircons in either alignment, all of the zircons probably crystallized at the same time (3840+30/-20 Ma) and experienced comparable subsequent histories. The lower intercept age of the younger alignment (2590+40/-80 Ma) reflects this later history but cannot be ascribed any particular geological significance given the well-documented presence of separate events of late-Archaean to Cambrian age affecting the Napier Complex (Grew *et al.* 1982, Black & James 1983, Black *et al.* 1983b 1987, Sheraton *et al.* 1987). The rather even spread of analyses on the probability distribution diagram (Fig. 4b) is unsuccessful at identifying a data maximum, except perhaps at *c.* 2450 Ma.

3000–2950 Ma orthogneiss

Black *et al.* (1986b) considered that charnockite (80285045) from Proclamation Island (Fig. 1) was emplaced during D_1–M_1 because of its fabric and approximate conformity with enclosing gneisses. A lack of mesoperthite and the presence of hornblende in the charnockite indicate that it did not form at the high temperatures seen in the Tula-Scott mountains regions. The zircons are complex (Appendix 1), with elongate igneous grains having been modified by metamorphic processes. ^{207}Pb/^{206}Pb ages range from 2490 Ma to 3000 Ma (Fig. 5a, b), but zircon morphology does not correlate with isotopic composition. Grain core ages do not relate to either

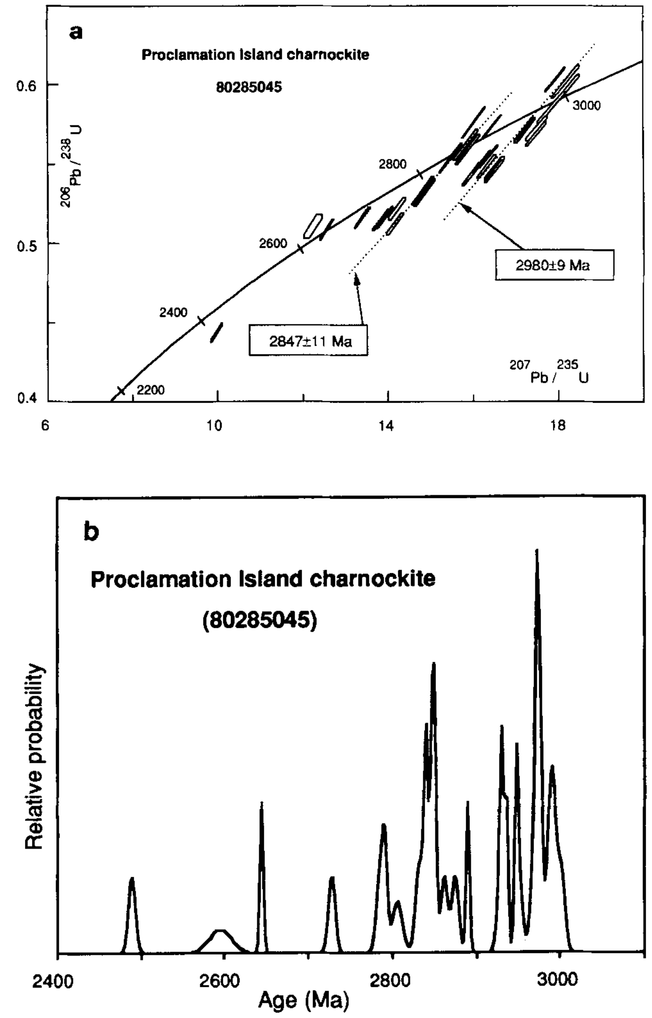

Fig. 5. a. ^{207}Pb/^{235}U–^{206}Pb/^{238}U concordia diagram for zircons from charnockite (80285045) at Proclamation Island. This rather complex data array is interpretable in terms of igneous crystallization at 2980±9 Ma and metamorphic resetting at 2847±11 Ma (see text). **b.** Probability distribution diagram showing two broad maxima in the upper age range, and a distinct tailing to younger values.

degree of zoning or U content, and rims span the entire range of ages. There are two main concentrations of ages (best shown on Fig. 5b), at 2980±9 Ma (9 analyses) and 2847±11 Ma (eight analyses). This type of isotopic array is consistent with most of the zircon crystallizing at the former time, and being subsequently affected by events at 2847±11 Ma, *c.* 2500 Ma and 1000 Ma (grain 12.1). This conclusion is largely consistent with the earlier conventional multigrain U–Pb zircon study of Black *et al.* (1986b).

An interesting feature of the Proclamation Island zircon data is that the Th/U ratios of all the analyses with ^{207}Pb/^{206}Pb ages in excess of 2940 Ma are clustered between 0.46 and 0.52. Although some of the zircons yielding younger ages have similar Th/U, most plot well outside this range (Fig. 6). This trend is consistent with growth of a 2980±9 Ma magmatic zircon population with a Th/U of *c.* 0.5. Differential movement of these elements subsequently occurred at the same time that radiogenic Pb was migrating from the zircon lattice. The correlation between Pb/U and Th/U (Table II) indicates that the U and Th migration was accompanied by a reasonably complementary migration of their respective daughter isotopes (^{206}Pb and ^{207}Pb for U, and ^{208}Pb for Th).

2850 Ma syn–UHT orthogneiss

A granitic orthogneiss (78285005) from Dallwitz Nunatak (Fig. 1) contains elongate zircons with partly rounded igneous terminations. Some grains consist of distinct cores surrounded by strongly zoned rims. Although the intensity of zoning correlates with U content, there is no correlation with isotopic composition. Forty analyses define a line with concordia intercepts at 2850+40/-20 Ma and 2500+140/-180 Ma (Fig. 7a), a feature that is also demonstrated by the probability distribution diagram (Fig. 7b). Both rounded cores and

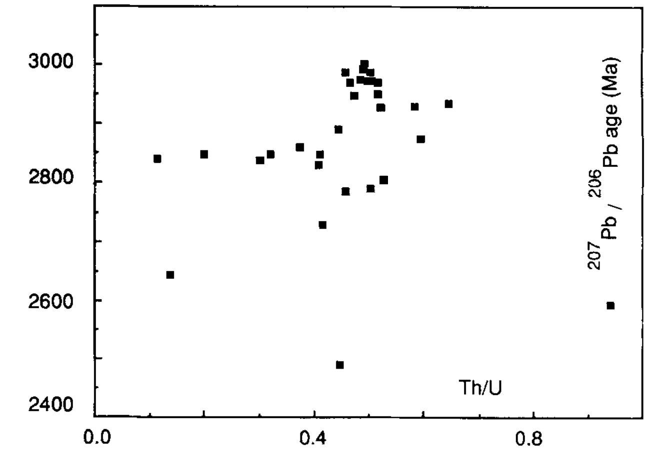

Fig. 6. Th/U–^{207}Pb/^{206}Pb-age diagram for zircons from the Proclamation Island charnockite (80285045). In contrast to the overall data array, all 11 analyses with ages exceeding 2940 Ma have a relatively constant Th/U of 0.46–0.52, which is possibly the primary magmatic value.

Table II. U–Th–Pb isotopic composition of zircons from the Napier Complex.

Grain area	U ($\mu g\ g^{-1}$)	Th ($\mu g\ g^{-1}$)	Th/U	$^{206}Pb/^{204}Pb$	$^{208}Pb/^{232}Th$ ±1 σ error	$^{206}Pb/^{238}U$ ±1 σ error	$^{207}Pb/^{235}U$ ±1 σ error	$^{207}Pb/^{206}Pb$ ±1 σ error	Age (Ma) ± 1 σ error	% conc
77283267 (Paragneiss, Mount Sones)										
11.1	1233	270	0.219	3926	0.0543±.0016	0.5734±.0104	15.49±.29	0.1959±.0005	2793±4	105
11.2	2075	1263	0.609	31 610	0.1642±.0030	0.6135±.0111	17.95±.33	0.2122±.0003	2922±2	106
12.1	2136	88	0.041	66 090	0.1530±.0033	0.6033±.0109	16.96±.31	0.2038±.0003	2857±2	107
12.2	940	25	0.027	52 360	0.1006±.0042	0.6020±.0109	17.36±.32	0.2092±.0005	2899±4	105
13.1	941	67	0.071	50 890	0.2281±.0049	0.9299±.0168	52.50±.96	0.4095±.0006	3944±2	107
14.1	1509	406	0.269	126 900	0.2414±.0045	0.9402±.0170	51.58±.94	0.3979±.0004	3901±2	110
15.1	362	444	1.229	29 450	0.1832±.0035	0.6925±.0127	24.74±.47	0.2591±.0009	3241±5	105
15.2	997	936	0.939	74 680	0.1720±.0031	0.6597±.0119	22.10±.41	0.2430±.0005	3139±3	104
15.3	472	632	1.338	199 200	0.1318±.0025	0.4789±.0087	10.87±.21	0.1646±.0007	2503±7	101
15.4	978	973	0.995	56 400	0.1672±.0031	0.6327±.0114	19.83±.37	0.2273±.0004	3033±3	104
16.1	1258	360	0.286	109 500	0.2420±.0045	0.9547±.0173	53.40±.98	0.4057±.0005	3930±2	110
17.1	761	68	0.089	33 110	0.1307±.0032	0.5913±.0107	18.13±.34	0.2223±.0005	2998±4	100
18.1	1192	578	0.485	75 080	0.2377±.0044	0.9969±.0181	60.22±1.11	0.4381±.0006	4045±2	110
19.1	992	602	0.607	85 400	0.1671±.0031	0.6198±.0112	18.56±.34	0.2172±.0005	2960±3	105
20.1	1263	713	0.565	4448	0.1222±.0023	0.5534±.0100	14.83±.27	0.1944±.0004	2780±4	102
21.1	697	67	0.096	32 200	0.1140±.0026	0.6616±.0120	20.77±.39	0.2277±.0005	3036±4	108
22.1	658	214	0.325	43 550	0.1501±.0028	0.5798±.0105	18.18±.34	0.2274±.0006	3034±4	97
23.1	245	339	1.380	11 560	0.1333±.0026	0.4812±.0088	10.85±.21	0.1636±.0009	2493±9	102
24.1	1313	58	0.044	14 650	0.1252±.0038	0.4828±.0087	10.73±.20	0.1612±.0004	2468±4	103
25.1	461	165	0.358	52 970	0.1559±.0030	0.5825±.0106	16.54±.31	0.2060±.0006	2874±5	103
77283465 (Orthogneiss, Mount Sones)										
1.1	416	107	0.258	14 880	0.2387±.0049	0.8808±.0161	46.22±.87	0.3806±.0009	3834±4	106
2.1	719	429	0.596	39 030	0.2414±.0045	0.8949±.0163	51.81±.96	0.4199±.0007	3982±3	103
3.1	1797	757	0.421	70 420	0.2034±.0037	0.7955±.0144	38.53±.70	0.3513±.0004	3712±2	102
4.1	765	601	0.786	46 360	0.2116±.0039	0.8337±.0152	46.16±.85	0.4016±.0007	3915±3	100
5.1	1261	286	0.227	41 050	0.1742±.0033	0.6401±.0116	24.51±.45	0.2777±.0005	3350±3	95
6.1	1017	436	0.428	52 100	0.2136±.0040	0.8423±.0153	44.65±.82	0.3845±.0006	3849±2	102
7.1	532	152	0.285	37 651	0.1856±.0036	0.7634±.0139	36.84±.69	0.3500±.0008	3707±3	99
8.1	651	260	0.400	40 060	0.2460±.0047	1.0623±.0193	65.46±1.21	0.4469±.0008	4075±3	114
9.1	2712	835	0.308	67 200	0.2127±.0039	0.8518±.0154	44.52±.81	0.3790±.0003	3828±1	104
10.1	898	205	0.228	10 500	0.1310±.0027	0.4868±.0088	11.48±.22	0.1711±.0007	2568±7	100
78285005 (Orthogneiss, Dallwitz Nunatak)										
1.1	347	229	0.659	12 600	0.1584±.0055	0.6077±.0206	18.57±.65	0.2216±.0010	2992±8	102
2.1	147	93	0.630	8087	0.1476±.0055	0.5337±.0182	14.53±.53	0.1974±.0017	2805±14	98
3.1	7968	1027	0.129	478 500	0.1779±.0060	0.6245±.0210	17.05±.58	0.1980±.0002	2809±2	111
3.2	2494	104	0.042	150 200	0.1414±.0051	0.5143±.0173	12.73±.43	0.1796±.0003	2649±3	101
4.1	2255	288	0.128	10 720	0.1660±.0058	0.6286±.0212	20.25±.69	0.2337±.0004	3077±3	102
5.1	1100	163	0.149	120 100	0.1558±.0054	0.5906±.0199	17.65±.60	0.2167±.0005	2956±4	101
5.2	2594	90	0.035	318 500	0.1520±.0054	0.5715±.0192	15.95±.54	0.2024±.0003	2846±3	102
6.1	969	89	0.092	36 670	0.1650±.0060	0.6932±.0233	30.76±1.05	0.3218±.0007	3579±3	95
7.1	965	87	0.090	52 630	0.1587±.0057	0.6134±.0207	19.84±.68	0.2346±.0006	3084±4	100
7.2	2023	77	0.038	137 900	0.1483±.0055	0.5517±.0186	15.31±.52	0.2013±.0004	2837±3	100
8.1	821	263	0.320	40 730	0.1538±.0053	0.5662±.0191	15.69±.54	0.2010±.0006	2834±5	102
9.1	208	207	0.999	77 520	0.1584±.0055	0.6019±.0204	17.56±.62	0.2116±.0012	2918±9	104
10.1	509	328	0.643	21 490	0.1638±.0056	0.5928±.0200	16.59±.57	0.2030±.0007	2850±6	105
10.2	1809	96	0.053	1351 000	0.1391±.0049	0.5236±.0176	13.59±.46	0.1882±.0004	2726±3	100
11.1	2140	1225	0.572	500 000	0.1518±.0051	0.5637±.0190	15.59±.53	0.2006±.0004	2831±3	102
11.2	2544	109	0.043	280 900	0.1275±.0045	0.4716±.0159	11.35±.39	0.1745±.0003	2602±3	96
12.1	1361	262	0.193	58 620	0.1216±.0042	0.4472±.0151	9.94±.34	0.1611±.0005	2468±5	97
13.1	702	58	0.083	62 700	0.1398±.0052	0.5730±.0193	15.25±.52	0.1930±.0006	2768±5	105
14.1	822	360	0.438	91 660	0.1711±.0058	0.6477±.0218	20.04±.68	0.2245±.0006	3013±4	107
14.2	2917	127	0.044	347 200	0.1339±.0047	0.5199±.0175	12.74±.43	0.1778±.0003	2632±3	103

The reported ages are derived from $^{207}Pb/^{206}Pb$ ratios. % conc is the relative concordance; values less than 100% plot below concordia, and values above 100% plot above it. Experimental procedures are given in Compston *et al.* (1984) and Williams *et al.* (1984).

Table II (continued). U–Th–Pb isotopic composition of zircons from the Napier Complex.

Grain area	U ($\mu g\ g^{-1}$)	Th ($\mu g\ g^{-1}$)	Th/U	$^{206}Pb/^{204}Pb$	$^{208}Pb/^{232}Th$ ±1 σ error	$^{206}Pb/^{238}U$ ±1 σ error	$^{207}Pb/^{235}U$ ±1 σ error	$^{207}Pb/^{206}Pb$ ±1 σ error	Age (Ma) ± 1 σ error	% conc
15.1	975	30	0.031	71 230	0.1345±.0060	0.5383±.0181	14.12±.48	0.1902±.0005	2744±5	101
15.2	1624	61	0.038	88 650	0.1433±.0054	0.5661±.0190	16.00±.54	0.2050±.0004	2866±4	101
16.1	2356	334	0.142	129 200	0.1319±.0045	0.4733±.0159	10.79±.37	0.1654±.0003	2511±4	99
17.1	2846	115	0.040	245 100	0.1431±.0050	0.5317±.0179	14.02±.48	0.1913±.0003	2753±3	100
17.2	2041	81	0.040	37 380	0.2079±.0076	0.5692±.0191	16.27±.55	0.2073±.0004	2885±3	101
18.1	622	288	0.464	61 280	0.1574±.0054	0.5894±.0199	17.71±.61	0.2179±.0008	2965±6	101
19.1	649	79	0.122	415 000	0.1417±.0052	0.5330±.0180	13.67±.47	0.1860±.0007	2707±7	102
19.2	1279	279	0.218	323 600	0.1276±.0044	0.4716±.0159	10.60±.36	0.1630±.0005	2487±6	100
20.1	3357	267	0.079	161 000	0.1554±.0053	0.5709±.0192	16.84±.57	0.2139±.0003	2935±3	99
20.2	2715	91	0.034	20 930	0.1199±.0050	0.4194±.0141	11.23±.38	0.1942±.0004	2778±4	81
21.1	960	286	0.298	69 640	0.1441±.0050	0.5278±.0178	14.28±.49	0.1962±.0006	2795±5	98
21.2	2208	82	0.037	13 680	0.1978±.0078	0.5043±.0170	12.80±.44	0.1841±.0004	2690±4	98
22.1	6410	539	0.084	3448 000	0.1362±.0046	0.4969±.0167	11.15±.38	0.1627±.0002	2484±2	105
23.1	650	223	0.344	1020 000	0.1472±.0051	0.5301±.0179	14.88±.51	0.2036±.0008	2855±6	96
23.2	1634	56	0.034	76 980	0.1744±.0067	0.5532±.0186	15.30±.52	0.2005±.0005	2831±4	100
24.1	759	341	0.450	99 400	0.1450±.0050	0.5505±.0186	15.77±.54	0.2077±.0008	2888±6	98
25.1	602	182	0.303	63 570	0.1501±.0053	0.5229±.0177	15.20±.53	0.2108±.0010	2911±7	93
25.2	2453	153	0.062	236 400	0.1213±.0043	0.4681±.0157	10.49±.36	0.1625±.0004	2482±5	100
26.1	684	241	0.352	58 140	0.1439±.0051	0.5668±.0192	16.46±.57	0.2106±.0010	2910±8	99
27.1	1535	42	0.027	176 700	0.1321±.0063	0.5070±.0171	13.18±.45	0.1885±.0006	2729±5	97
28.1	2248	908	0.404	769 200	0.1476±.0050	0.5607±.0189	15.59±.53	0.2016±.0005	2839±4	101
29.1	1046	359	0.344	119 600	0.1227±.0042	0.4546±.0153	10.12±.35	0.1614±.0007	2470±7	98
30.1	882	265	0.300	75 300	0.1187±.0042	0.4511±.0152	10.16±.35	0.1633±.0008	2490±9	96
					78285007 (Orthogneiss, Mount Sones)					
1.1	283	161	0.569	485 400	0.2278±.0070	0.9399±.0284	59.32±1.81	0.4578±.0008	4111±3	104
1.2	340	226	0.666	199 200	0.2121±.0065	0.8864±.0267	53.55±1.63	0.4381±.0007	4045±2	101
1.3	304	263	0.866	460 800	0.2107±.0064	0.8723±.0263	48.08±1.47	0.3997±.0007	3908±3	103
1.4	256	63	0.247	59 630	0.1995±.0064	0.8806±.0266	50.16±1.53	0.4131±.0009	3957±3	103
1.5	247	58	0.235	6250 000	0.1878±.0059	0.8705±.0263	48.07±1.47	0.4005±.0008	3911±3	103
1.6	268	144	0.538	78 190	0.2282±.0070	0.9438±.0285	57.02±1.74	0.4382±.0009	4046±3	106
2.1	85	50	0.588	57 830	0.2436±.0080	1.0321±.0317	67.78±2.12	0.4763±.0014	4170±4	110
2.2	93	52	0.563	1887 000	0.2005±.0064	0.7863±.0240	43.44±1.35	0.4007±.0012	3912±5	96
2.3	73	44	0.599	126 900	0.2389±.0079	0.9863±.0303	59.10±1.85	0.4346±.0015	4033±5	110
2.4	88	57	0.643	134 800	0.2124±.0070	0.9217±.0283	52.93±1.66	0.4165±.0016	3970±6	106
2.5	97	59	0.615	1000 000	0.1982±.0064	0.8320±.0254	45.17±1.40	0.3938±.0014	3885±5	100
3.1	167	77	0.458	88 260	0.1817±.0058	0.7352±.0223	32.31±1.00	0.3188±.0009	3564±5	100
3.2	129	61	0.472	38 900	0.1891±.0061	0.7619±.0232	37.14±1.15	0.3536±.0012	3722±5	98
3.3	395	69	0.176	196 900	0.1835±.0059	0.7670±.0231	35.88±1.09	0.3393±.0007	3659±3	100
4.1	497	379	0.761	226 800	0.2061±.0063	0.8318±.0250	45.63±1.38	0.3979±.0005	3901±2	100
4.2	363	182	0.500	28 110	0.2017±.0062	0.8574±.0259	45.96±1.40	0.3888±.0007	3866±3	103
5.1	206	80	0.390	487 800	0.2500±.0078	1.0897±.0330	67.98±2.08	0.4524±.0008	4093±3	116
5.2	118	52	0.442	1000 000	0.1921±.0062	0.7850±.0239	38.87±1.20	0.3591±.0011	3746±5	100
5.3	152	69	0.452	289 900	0.2158±.0068	0.9158±.0278	47.43±1.46	0.3756±.0009	3814±4	110
6.1	116	69	0.588	48 450	0.1884±.0060	0.7951±.0242	41.36±1.28	0.3773±.0011	3821±4	99
6.2	184	150	0.813	23 710	0.2068±.0064	0.8772±.0266	49.15±1.51	0.4063±.0010	3933±4	103
7.1	102	50	0.484	78 430	0.2438±.0079	1.0165±.0310	61.43±1.90	0.4383±.0012	4046±4	112
7.2	53	26	0.485	273 200	0.2082±.0071	0.8584±.0265	45.54±1.44	0.3848±.0016	3851±6	104
8.1	197	111	0.562	47 150	0.2064±.0064	0.8548±.0259	46.32±1.42	0.3930±.0009	3882±3	103
8.2	207	108	0.521	43 230	0.2240±.0070	0.9237±.0279	53.57±1.64	0.4206±.0008	3984±3	106
8.3	288	96	0.333	1000 000	0.1976±.0061	0.8061±.0243	41.71±1.27	0.3753±.0007	3813±3	100
					78285013 (Orthogneiss, Gage Ridge)					
1.1	1949	131	0.067	57 440	0.1403±.0044	0.5383±.0156	15.52±.45	0.2090±.0003	2898±2	96
2.1	2378	204	0.086	53 620	0.1370±.0042	0.5231±.0152	13.96±.41	0.1935±.0002	2773±2	98
3.1	3754	254	0.068	25 010	0.1765±.0054	0.6787±.0197	27.76±.81	0.2966±.0002	3453±1	97
4.1	1068	81	0.076	581 400	0.1610±.0050	0.5828±.0170	19.34±.57	0.2407±.0004	3124±2	95

The reported ages are derived from $^{207}Pb/^{206}Pb$ ratios. % conc is the relative concordance; values less than 100% plot below concordia, and values above 100% plot above it. Experimental procedures are given in Compston *et al.* (1984) and Williams *et al.* (1984).

Table II (continued). U–Th–Pb isotopic composition of zircons from the Napier Complex.

Grain area	U ($\mu g\ g^{-1}$)	Th ($\mu g\ g^{-1}$)	Th/U	$^{206}Pb/^{204}Pb$	$^{208}Pb/^{232}Th$ ±1 σ error	$^{206}Pb/^{238}U$ ±1 σ error	$^{207}Pb/^{235}U$ ±1 σ error	$^{207}Pb/^{206}Pb$ ±1 σ error	Age (Ma) ± 1 σ error	% conc
5.1	477	285	0.597	458 700	0.2217±.0066	0.9185±.0269	57.14±1.69	0.4512±.0008	4089±3	103
5.2	637	440	0.691	68 450	0.2240±.0066	0.9215±.0269	56.75±1.67	0.4467±.0006	4074±2	103
5.3	280	135	0.481	26 260	0.2308±.0070	0.9735±.0285	61.69±1.83	0.4596±.0009	4116±3	106
6.1	1459	517	0.354	72 890	0.2343±.0069	0.7834±.0228	39.61±1.16	0.3668±.0004	3778±2	99
7.1	1590	260	0.163	94 250	0.1759±.0052	0.6847±.0199	29.91±.87	0.3168±.0003	3554±2	95
8.1	1721	284	0.165	18 620	0.1402±.0042	0.4885±.0142	10.96±.32	0.1627±.0002	2484±3	103
9.1	2123	144	0.068	240 400	0.1315±.0040	0.4951±.0144	11.84±.35	0.1735±.0002	2591±2	100
10.1	1711	87	0.051	137 600	0.1376±.0043	0.5164±.0150	13.37±.39	0.1878±.0002	2723±2	99
11.1	1968	331	0.168	197 200	0.1268±.0037	0.4681±.0136	10.48±.31	0.1624±.0002	2480±2	100
12.1	2528	168	0.067	198 000	0.1488±.0045	0.5682±.0165	18.15±.53	0.2316±.0002	3063±2	95
13.1	4963	346	0.070	330 000	0.1306±.0039	0.4847±.0141	10.88±.32	0.1627±.0001	2484±1	103
13.2	2351	415	0.176	41 190	0.1214±.0036	0.4706±.0137	10.60±.31	0.1634±.0002	2491±2	100
14.1	3441	326	0.095	120 200	0.1736±.0051	0.6655±.0193	25.99±.76	0.2833±.0002	3381±1	97
15.1	1997	106	0.053	36 180	0.1856±.0058	0.7283±.0212	33.04±.96	0.3290±.0003	3612±1	98
16.1	2053	152	0.074	123 300	0.1364±.0042	0.5209±.0151	13.25±.39	0.1845±.0002	2694±2	100
17.1	1899	269	0.142	113 100	0.1467±.0043	0.5653±.0164	18.72±.55	0.2402±.0003	3121±2	93
18.1	3611	1347	0.373	740 700	0.2018±.0059	0.7912±.0230	38.93±1.13	0.3569±.0002	3737±1	101
18.2	1265	215	0.170	62 810	0.1230±.0037	0.4487±.0130	10.07±.30	0.1628±.0003	2485±3	96
19.1	3472	1319	0.380	714 300	0.2150±.0063	0.8605±.0250	45.57±1.33	0.3841±.0002	3848±1	104
20.1	1635	113	0.069	5740	0.1468±.0053	0.5714±.0166	18.26±.53	0.2318±.0003	3065±2	95
21.1	2344	170	0.073	21 430	0.1765±.0054	0.5781±.0168	19.18±.56	0.2406±.0003	3124±2	94
22.1	134	51	0.380	59 030	0.1519±.0051	0.5850±.0173	23.20±.70	0.2877±.0012	3405±7	87
23.1	2552	546	0.214	181 200	0.1905±.0056	0.7030±.0204	32.29±.94	0.3331±.0003	3631±1	95
24.1	2244	2288	1.020	358 400	0.2155±.0063	0.8714±.0253	46.54±1.36	0.3874±.0003	3861±1	105
24.2	727	806	1.109	40 270	0.2198±.0064	0.8442±.0246	41.96±1.23	0.3605±.0005	3752±2	105
25.1	3805	1003	0.264	602 400	0.1906±.0056	0.7213±.0209	31.45±.92	0.3162±.0002	3552±1	99
26.1	1508	76	0.050	11 110 000	0.1300±.0040	0.4818±.0140	11.09±.32	0.1669±.0002	2527±3	100
27.1	289	105	0.363	1264	0.1954±.0069	0.7367±.0216	34.60±1.03	0.3406±.0011	3666±5	97
28.1	717	205	0.287	31 580	0.2250±.0067	0.8565±.0249	48.23±1.41	0.4084±.0006	3940±2	101
28.2	1294	64	0.049	404 900	0.1383±.0043	0.5323±.0155	13.96±.41	0.1903±.0003	2744±2	100
29.1	1591	113	0.071	151 500	0.1458±.0045	0.5665±.0165	18.06±.53	0.2312±.0003	3061±2	95
30.1	2642	209	0.079	657 900	0.1459±.0043	0.5613±.0163	17.01±.50	0.2198±.0002	2979±2	96
31.1	1912	154	0.081	241 000	0.1478±.0045	0.5661±.0164	17.46±.51	0.2237±.0003	3007±2	96
32.1	1649	425	0.258	14 140	0.1471±.0044	0.5624±.0163	17.97±.53	0.2317±.0003	3064±2	94
33.1	824	45	0.055	8984	0.1987±.0078	0.7226±.0210	31.33±.92	0.3145±.0005	3543±2	99
34.1	694	268	0.387	76 630	0.2056±.0061	0.7971±.0232	43.09±1.26	0.3921±.0005	3879±2	97
					80285037 (Paragneiss, Zircon Point)					
1.1	316	114	0.360	12 040	0.1327±.0045	0.4860±.0147	13.15±.41	0.1963±.0007	2795±6	91
2.1	498	184	0.370	14 700	0.1046±.0034	0.4033±.0122	8.52±.26	0.1532±.0005	2381±6	92
3.1	1206	173	0.143	58 790	0.1209±.0040	0.4024±.0121	8.61±.26	0.1552±.0004	2404±4	91
4.1	2007	988	0.492	109 900	0.1442±.0046	0.5513±.0166	14.95±.45	0.1967±.0003	2799±2	101
4.2	483	221	0.456	191 900	0.1369±.0045	0.5356±.0162	14.42±.44	0.1952±.0006	2787±5	99
5.1	1394	692	0.496	53 330	0.1388±.0044	0.5369±.0161	14.20±.43	0.1918±.0003	2758±3	100
5.2	221	391	1.764	17 360	0.1236±.0040	0.4674±.0142	10.50±.33	0.1629±.0008	2486±9	99
6.1	376	149	0.395	27 110	0.1469±.0048	0.5516±.0166	16.64±.51	0.2188±.0005	2972±4	95
6.2	331	144	0.436	29 470	0.1295±.0042	0.4583±.0138	10.51±.32	0.1664±.0004	2521±4	96
7.1	858	337	0.393	64 390	0.1412±.0045	0.5261±.0158	14.66±.44	0.2021±.0003	2843±3	96
7.2	725	159	0.219	25 430	0.1279±.0042	0.4579±.0138	10.52±.32	0.1666±.0004	2524±4	96
8.1	908	500	0.550	432 900	0.1311±.0042	0.4955±.0149	12.55±.38	0.1836±.0003	2686±3	97
9.1	895	410	0.458	48 900	0.1443±.0046	0.5580±.0168	15.98±.48	0.2077±.0003	2888±3	99
9.2	1265	547	0.433	240 400	0.1429±.0046	0.5610±.0169	15.70±.48	0.2029±.0003	2850±3	101
10.1	573	206	0.360	40 190	0.1283±.0041	0.4869±.0146	11.42±.35	0.1702±.0004	2559±4	100
10.2	551	195	0.354	55 900	0.1291±.0042	0.4943±.0149	11.75±.36	0.1723±.0004	2580±4	100
11.1	378	35	0.092	22 010	0.1403±.0055	0.5443±.0164	14.97±.46	0.1995±.0005	2822±4	99
12.1	608	228	0.375	51 280	0.1293±.0042	0.4875±.0147	11.56±.35	0.1719±.0004	2577±4	99
13.1	927	250	0.270	263 900	0.1207±.0039	0.4617±.0139	10.66±.32	0.1674±.0003	2532±3	97

The reported ages are derived from $^{207}Pb/^{206}Pb$ ratios. % conc is the relative concordance; values less than 100% plot below concordia, and values above 100% plot above it. Experimental procedures are given in Compston *et al.* (1984) and Williams *et al.* (1984).

https://doi.org/10.1017/S0954102097000102 Published online by Cambridge University Press

Table II (continued). U–Th–Pb isotopic composition of zircons from the Napier Complex.

Grain area	U (μg g^{-1})	Th (μg g^{-1})	Th/U	^{206}Pb/^{204}Pb	^{208}Pb/^{232}Th ±1 σ error	^{206}Pb/^{238}U ±1 σ error	^{207}Pb/^{235}U ±1 σ error	^{207}Pb/^{206}Pb ±1 σ error	Age (Ma) ± 1 σ error	% conc
14.1	512	119	0.233	29 310	0.0980±.0033	0.3735±.0113	7.17±.22	0.1393±.0005	2218±6	92
15.1	385	133	0.345	33 860	0.1411±.0046	0.5571±.0168	15.58±.48	0.2028±.0006	2849±5	100
16.1	497	215	0.433	48 150	0.1257±.0041	0.4819±.0145	11.74±.36	0.1768±.0005	2623±4	97
17.1	493	185	0.376	241 500	0.0965±.0031	0.3558±.0107	6.95±.21	0.1417±.0004	2249±5	87
18.1	474	204	0.431	11 770	0.0955±.0031	0.3520±.0106	6.23±.19	0.1284±.0005	2076±8	94
19.1	448	195	0.435	328 900	0.1482±.0048	0.5659±.0171	16.23±.50	0.2081±.0006	2891±4	100
20.1	1169	612	0.524	39 760	0.1433±.0046	0.5504±.0166	15.21±.46	0.2004±.0003	2829±3	100
21.1	1725	729	0.422	223 200	0.1491±.0048	0.5822±.0175	16.29±.49	0.2030±.0003	2850±3	104
22.1	1639	781	0.477	4545 000	0.1449±.0046	0.5658±.0170	15.70±.48	0.2012±.0003	2836±3	102
23.1	474	187	0.395	392 200	0.1453±.0047	0.5643±.0171	15.93±.49	0.2047±.0006	2864±5	101
24.1	1110	591	0.533	369 000	0.1403±.0045	0.5419±.0163	14.91±.45	0.1996±.0003	2823±3	99
25.1	667	285	0.428	48 120	0.1380±.0045	0.5360±.0162	14.51±.44	0.1963±.0005	2795±4	99
26.1	301	139	0.461	27 890	0.1375±.0048	0.5517±.0168	14.75±.46	0.1939±.0010	2776±8	102
26.2	856	346	0.405	60 610	0.1325±.0044	0.5051±.0152	11.41±.35	0.1638±.0006	2495±6	106
27.1	429	195	0.454	283 300	0.1423±.0046	0.5579±.0168	15.55±.48	0.2022±.0006	2844±5	100
27.2	607	238	0.392	100 000	0.1195±.0042	0.4548±.0137	10.46±.33	0.1668±.0008	2525±8	96
28.1	796	347	0.436	75 470	0.1300±.0043	0.5030±.0152	11.46±.35	0.1653±.0006	2510±6	105
29.1	809	207	0.256	137 600	0.1208±.0040	0.4599±.0139	9.86±.30	0.1555±.0005	2408±5	101
30.1	1407	625	0.444	126 700	0.1394±.0044	0.5490±.0165	14.02±.42	0.1852±.0003	2700±3	104
31.1	572	127	0.222	32 100	0.1321±.0044	0.4878±.0147	11.88±.36	0.1766±.0005	2621±4	98
					80285045 (Charnockite, Proclamation Island)					
1.1	746	278	0.373	21 860	0.1544±.0030	0.5621±.0098	15.84±.28	0.2044±.0005	2862±4	100
1.2	807	480	0.595	12 470	0.1607±.0030	0.5593±.0097	15.89±.28	0.2061±.0005	2875±4	100
1.3	700	211	0.302	15 950	0.1506±.0031	0.5334±.0092	14.83±.26	0.2016±.0005	2839±4	97
2.1	1217	139	0.114	98 040	0.1571±.0029	0.5762±.0098	16.03±.28	0.2017±.0002	2840±2	103
2.2	318	145	0.457	18 000	0.1629±.0031	0.5961±.0103	18.18±.32	0.2211±.0005	2989±4	101
3.1	496	248	0.500	23 000	0.1613±.0029	0.6017±.0104	18.18±.32	0.2191±.0004	2974±3	102
3.2	765	314	0.411	35 660	0.1509±.0027	0.5540±.0095	15.49±.27	0.2027±.0003	2848±3	100
4.1	348	175	0.503	22 950	0.1549±.0029	0.5857±.0101	17.85±.32	0.2211±.0005	2988±4	99
4.2	451	188	0.417	26 350	0.1473±.0022	0.5164±.0069	13.41±.18	0.1883±.0004	2728±4	98
5.1	304	157	0.517	5170	0.1519±.0025	0.5474±.0074	16.51±.24	0.2187±.0007	2971±5	95
6.1	348	182	0.523	23 930	0.1495±.0023	0.5437±.0073	15.97±.22	0.2130±.0005	2929±4	96
6.2	287	134	0.468	31 480	0.1588±.0026	0.5714±.0078	17.23±.25	0.2187±.0006	2971±5	98
6.3	412	201	0.487	57 340	0.1487±.0022	0.5454±.0073	16.50±.23	0.2194±.0005	2976±3	94
7.1	830	484	0.583	83 750	0.1513±.0021	0.5515±.0073	16.21±.22	0.2132±.0003	2930±2	97
7.2	881	568	0.645	74 350	0.1542±.0021	0.5549±.0073	16.37±.22	0.2140±.0003	2936±2	97
8.1	318	130	0.408	16 020	0.1395±.0023	0.5125±.0069	14.18±.20	0.2006±.0005	2831±4	94
9.1	758	384	0.507	67 070	0.1568±.0022	0.5705±.0075	17.22±.23	0.2189±.0003	2972±2	98
10.1	299	147	0.493	29 700	0.1553±.0024	0.5689±.0076	17.49±.24	0.2229±.0005	3002±4	97
11.1	1473	656	0.446	65 450	0.1578±.0021	0.5736±.0075	16.44±.22	0.2079±.0002	2890±2	101
12.1	453	202	0.447	21 030	0.1209±.0018	0.4437±.0059	9.99±.14	0.1632±.0004	2489±4	95
12.2	274	145	0.527	4032	0.1449±.0025	0.5223±.0071	14.23±.20	0.1976±.0007	2806+6	97
13.1	509	256	0.504	36 090	0.1442±.0021	0.5165±.0068	13.94±.19	0.1957±.0003	2791±3	96
13.2	261	135	0.518	18 920	0.1520±.0024	0.5483±.0074	16.33±.23	0.2161±.0005	2951±4	95
14.1	241	119	0.492	11 340	0.1568±.0026	0.5722±.0077	17.50±.25	0.2219±.0006	2994±4	97
15.1	456	91	0.201	43 330	0.1479±.0024	0.5306±.0070	14.84±.20	0.2028±.0004	2849±3	96
16.1	359	115	0.320	42 900	0.1576±.0024	0.5335±.0071	14.92±.20	0.2029±.0004	2849±3	97
17.1	328	150	0.459	19 180	0.1388±.0022	0.5151±.0069	13.85±.19	0.1951±.0005	2785±4	96
18.1	978	465	0.475	34 310	0.1533±.0021	0.6032±.0079	17.93±.24	0.2156±.0003	2948±2	103
19.1	102	95	0.940	4037	0.1404±.0028	0.5107±.0074	12.24±.21	0.1739±.0013	2595±13	102
20.1	1022	141	0.138	70 080	0.1322±.0020	0.5088±.0067	12.56±.17	0.1791±.0002	2644±2	100

The reported ages are derived from ^{207}Pb/^{206}Pb ratios. % conc is the relative concordance; values less than 100% plot below concordia, and values above 100% plot above it. Experimental procedures are given in Compston *et al.* (1984) and Williams *et al.* (1984).

zoned zircon rims yield ages up to 2850 Ma, the age ascribed to the syn-deformational igneous crystallization of the precursor to the gneiss. All nine analyses with Th/U greater than 0.4 have relatively old ^{207}Pb/^{206}Pb ages (i.e. exceeding 2800 Ma). The core of one zircon grain (6.1) is considerably older than any of the other analysed grains and its isotopic

https://doi.org/10.1017/S0954102097000102 Published online by Cambridge University Press

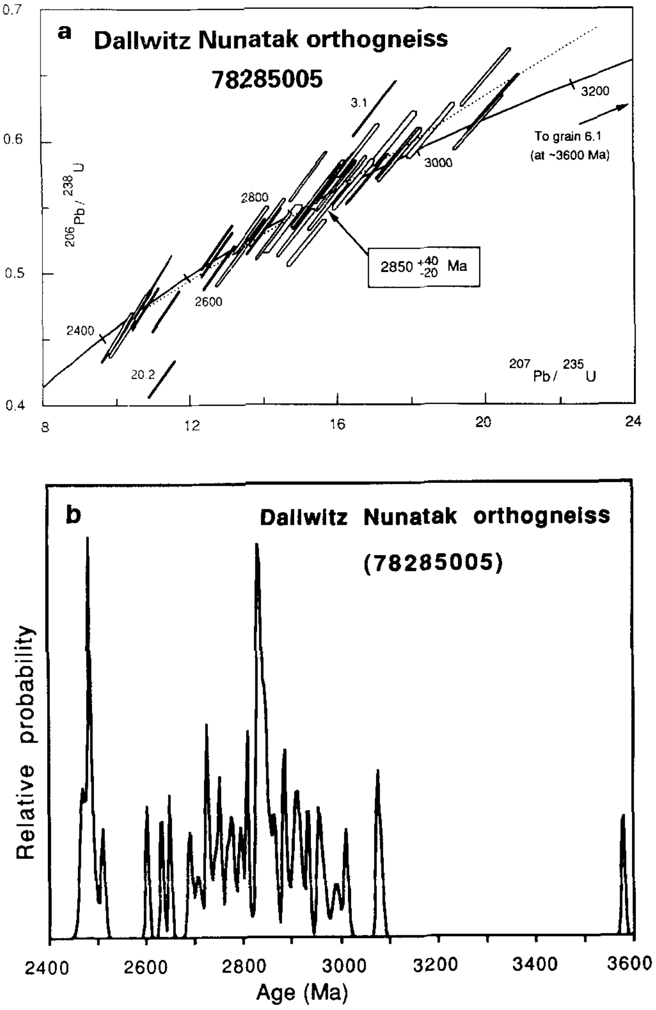

Fig. 7. a. $^{207}Pb/^{235}U$–$^{206}Pb/^{238}U$ concordia diagram for zircons from orthogneiss (78285005) at Dallwitz Nunatak. All but three of the analyses are consistent with a crystallization age of 2850+40/-20 Ma for the granitic precursor of this gneiss. Grain 6.1 crystallized considerably earlier. Analysis 3.1 probably plots above the main group because of its high U content and related radiation damage. b. There is good agreement between the concordia intercept ages and the maxima on the probability distribution diagram.

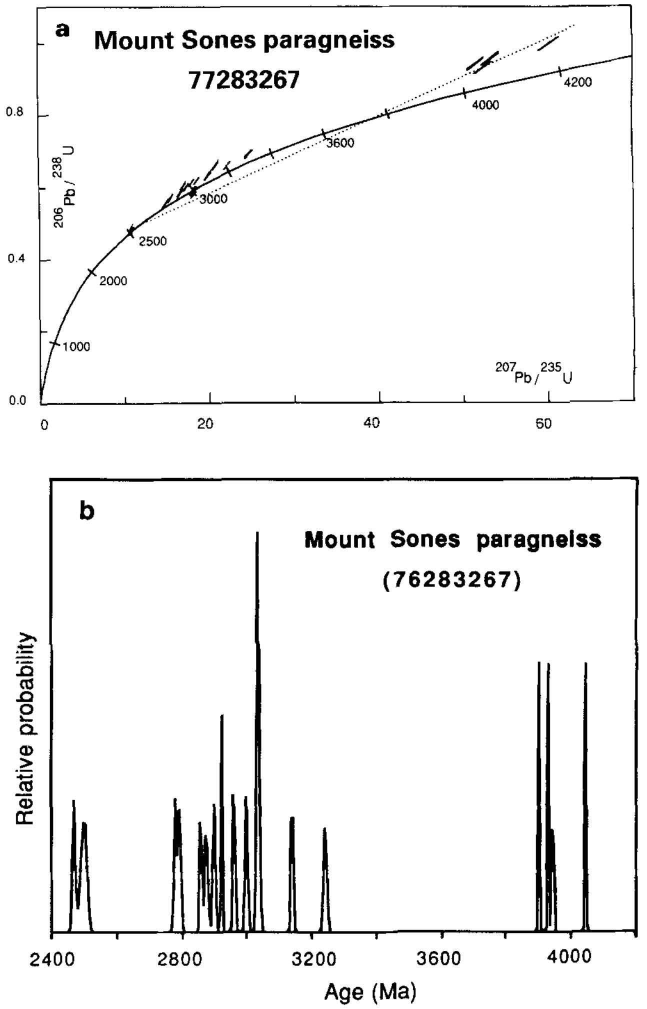

Fig. 8. a. $^{207}Pb/^{235}U$–$^{206}Pb/^{238}U$ concordia diagram for zircons from paragneiss (77283267) at Mount Sones. Their isotopic composition is consistent with the sedimentary precursor of this gneiss being at least partly derived from nearby orthogneisses. b. The probability distribution diagram shows the age range at the lower end of concordia a little more clearly.

composition is similar to that of the older grains in the Mount Sones and Gage Ridge orthogneisses. This minor component of the zircon population in the Dallwitz Nunatak orthogneiss is considered to be of xenocrystic origin.

The younger age intercept (2500 Ma) reflects partial isotopic resetting during subsequent tectonothermal events. Six analyses including equant multifaceted grains of typical metamorphic morphology, two zoned rims and an unusual stubby euhedral grain give a best-fit, concordant ($^{207}Pb/^{206}Pb$) age of 2481±4 Ma. This is similar to that ascribed to D3 in previous studies (Black & James 1983, Black *et al.* 1983a, Sheraton *et al.* 1987), and is also coincident with the *c.* 2500 Ma age preferred by Grew *et al.* (1982) and Sandiford and Wilson (1984) for the highest grade metamorphism in the Napier Complex.

Paragneisses

Zircons from a paragneiss (77283267) at Mount Sones (Fig. 1) were analysed for comparison with those from the nearby orthogneisses analysed above. The zircons have a wide range of isotopic compositions ($^{207}Pb/^{235}U$ ranges from 11–60), which appear to form two groups (Fig. 8a). Four of the grains (13.1, 14.1, 16.1 and 18.1) have $^{207}Pb/^{206}Pb$ ages between 3900 Ma and 4050 Ma and may have been derived from a protolith similar to that of the Mount Sones orthogneiss itself. The remaining 16 grains define a linear trend (MSWD = 4.8) along concordia from *c.* 3240–2470 Ma. However,

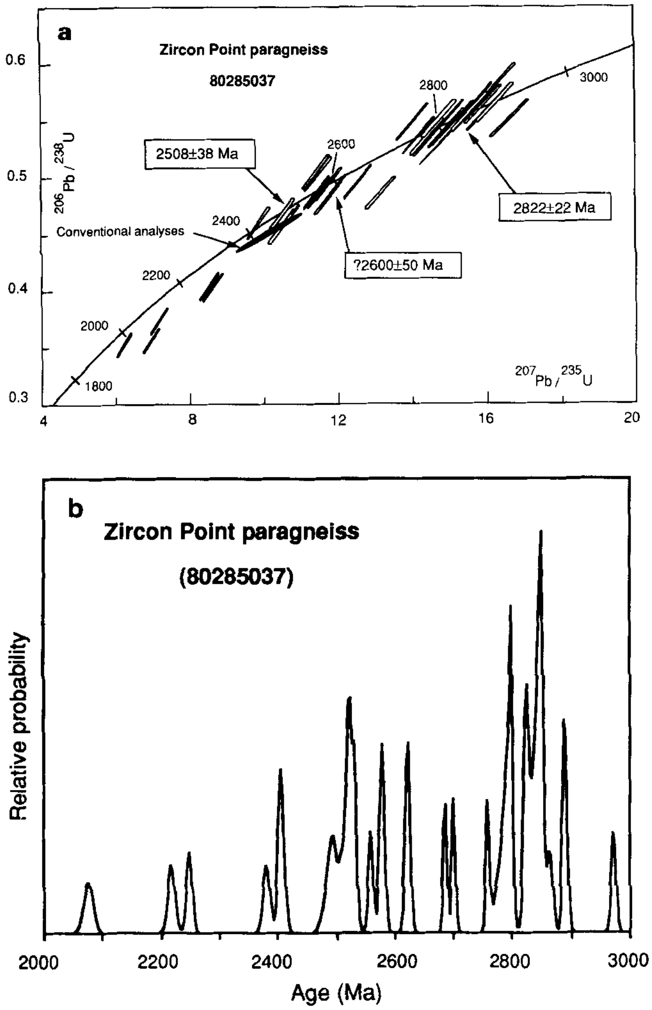

Fig. 9. a. $^{207}Pb/^{235}U$–$^{206}Pb/^{238}U$ concordia diagram for zircons from paragneiss (80285037) at Zircon Point, showing no evidence of the 3000 Ma and 3800 Ma grains that are characteristic of the more easterly part of the Napier Complex. However, two (and perhaps three) younger populations are present. The solid, narrow oval field depicts the full range of six conventional multigrain analyses, illustrating how that technique averages out the isotopic characteristics of zircon populations. **b.** Probability distribution diagram showing the symmetrical spread of analyses about an age between 2800–2900 Ma, and a separate data concentration at *c.* 2500 Ma.

their proximity to, and sub-parallel trend with, concordia do not allow the derivation of meaningful intercept ages. Several interpretations of the data are possible, including derivation from the old but modified orthogneisses, derivation from younger orthogneisses, or modification by metamorphic annealing between 3000–2500 Ma. At least two of the three analyses (15.3, 23.1 and 24.1), with ages of *c.* 2500 Ma, represent zircon that has been metamorphically reset, and not new metamorphic growth at that time. The corresponding probability distribution diagram (Fig. 8b) is no more successful at resolving trends in the data.

Zircons from paragneiss (80285037) at Zircon Point in Khmara Bay (Fig. 1) form a different isotopic array (Fig. 9a), with no evidence of zircon ages of 3000 Ma or more. They define several ages groups that have no clear correlation with grain morphology or degree of internal zoning. Nineteen near-concordant analyses define a concordant, mean $^{207}Pb/^{206}Pb$ age of 2822±22 Ma, similar to that (2850+40/-20 Ma) derived from the Dallwitz Nunatak orthogneiss. Six slightly discordant analyses (5.2, 6.2, 7.2, 13.1, 27.2 and 29.1) group near the opposite end of the age spectrum at 2508±38 Ma ($^{207}Pb/^{206}Pb$). Although a group of eight analyses with a mean $^{207}Pb/^{206}Pb$ age of 2600±50 Ma might indicate an unsuspected ~2600 Ma event, it is more likely that they reflect a grouping of 2850 grains that were partially reset at ~2500 Ma. Conventional analyses of the zircons in this paragneiss (Black *et al.* 1983b) had obscured the isotopic heterogeneities noted above. The probability distribution diagram (Fig. 9b) also shows the symmetrical data concentration at *c.* 2800 Ma and that at *c.* 2500 Ma.

Discussion

Age and extent of the earliest Napier Complex rocks

The new SHRIMP data confirm the presence of Early Archaean crust in the Napier Complex, but indicate that it is almost certainly not as ancient as proposed by Ravich *et al.* (1975), Sobotovich *et al.* (1976), Lovering (1979, 1980) and Black *et al.* (1986a). The reasons that the earliest of those studies yield erroneous ages are summarized in Black *et al.* (1983a), and the *c.* 100 Ma overestimate for the age of this event by Black *et al.* (1986a) is largely a result of an inappropriate normalization of Pb/U, as explained above. The Gage Ridge orthogneiss and those at Mount Sones are remnants of this early crust, and their igneous precursors crystallized between 3840 Ma and 3770 Ma, with the precursors of the Gage Ridge orthogneiss being marginally older than those at Mt Sones. The minimum time interval for this early magmatic activity is 34 million years (3820 to 3786 Ma based on 2-σ errors).

Conventional multigrain zircon U–Pb data (Black *et al.* 1983a, Black & James 1983) and reconnaissance SHRIMP results (Compston & Williams 1982) suggested that orthogneiss at Fyfe Hills is of comparable antiquity. However, zircons in the Fyfe Hills samples preserve far less memory of that age than those from the Mount Sones and Gage Ridge orthogneisses. The fact that average zircon ages are not even as old as 2700 Ma for gneisses from several peaks in the Tula and Scott mountains (LPB, unpublished reconnaissance multigrain U–Pb analyses: Mount Tod, Grimsley Peak, Mount Hardy, Mount Riiser-Larsen and Mount George) suggests that 3800 Ma gneiss precursors are probably in the minority in the Napier Complex, even allowing for the possibility that old zircons will have lost a considerable proportion of their radiogenic Pb.

Detrital zircons from paragneisses provide a useful

https://doi.org/10.1017/S0954102097000102 Published online by Cambridge University Press

additional source of information on the ages of exposed crustal protoliths that were sourcing sediments (e.g. Froude *et al.* 1983, Kinny 1986). Although limited in scope and coverage, the contrasting zircon isotopic data reported here for the Mount Sones and Zircon Point paragneisses suggest that supracrustal rocks in the Napier Complex have a complex history that will only be understood through further isotopic studies tied to systematic sampling of paragneiss sequences. The analysed Mount Sones paragneiss contains four grains of comparable age to the oldest ones in the orthogneiss, and the overall isotopic similarity of the zircon in both rocks is consistent with the paragneiss precursor being derived, at least in part, from the precursor of the orthogneiss. An additional, considerably younger (*c.* 3100 Ma) source may explain the morphological range of the zircons in this paragneiss, and would require deposition of the sedimentary precursor only shortly before the *c.* 2980 Ma D_1–M_1 event. In contrast to the Mount Sones paragneiss, the Zircon Point paragneiss lacks 3000 Ma or older zircons despite the proximity of this paragneiss to the Fyfe Hills, where ancient crust of *c.* 3700 Ma apparently exists (Black *et al.* 1983a, DePaolo *et al.* 1982, Lovering 1980, Sobotovich *et al.* 1976). This suggests that the old crust was not exposed, or at least not providing a source for the sediments in the Khmara Bay area. As the general paragneiss sequence in Khmara Bay, which includes sillimanite metapelites and orthopyroxene-sillimanite quartzites, and sapphirine-quartz rocks, is comparable to many paragneisses in Amundsen Bay (e.g. East Tonagh Island, Harley 1987) the young ages for detrital zircons in this paragneiss support the conclusion that the very old crustal precursors form only a minor component of the exposed crust in the Napier Complex compared with rocks formed at or after 3000 Ma.

The new *c.* 3800 Ma dates for the Tula Mountains orthogneisses make them comparable in age to several other Archaean high grade terrains, and provide further credence for that time period being an important one for continental crustal growth. Most notably, much of the Amitsoq Gneiss (Nutman *et al.* 1993) and the Isua supracrustal belt (Compston *et al.* 1986, Kinny 1986) of southern West Greenland are similar in age, and precursor source rocks 3863±12 Ma in age have been deduced from xenocrystic zircons in the 3732±6 Ma Uivak gneisses of northern Labrador (Schiotte *et al.* 1989). Detrital 3800 Ma zircons from metasediments suggest that parts of the Sino-Korean craton (Liu *et al.* 1992) are also of comparable age.

Deformation-metamorphic events in the Napier Complex

Until now, we have adopted the D_1, D_2 and D_3 terminology of Black & James (1983) and James & Black (1981), which was developed in particular to describe the structural evolution of the Amundsen Bay region. D_1 was defined as the principal fabric-forming event to have produced isoclinal folds, intense mineral-elongation lineations, and strong layer-parallel gneissic fabrics defined by granulite-facies assemblages. This deformation was responsible for the interleaving and parallelism of the various ortho- and paragneiss components. D_2 deformation progressed under similar high-grade granulite-facies conditions to D_1 and produced tight to isoclinal folds with local S_2 fabrics. D_3–M_3 produced upright to steeply-inclined folds under less severe metamorphic conditions (700°C, 0.5–0.8 GPa). In all but the extreme southwest of the Napier Complex, S_3 fabrics are only locally developed (Black & James 1983, Sandiford & Wilson 1984). Where observed, these fabrics involve modification of earlier granoblastic or elongate fabrics by superposed intracrystalline deformation and grain-boundary recrystallization. As noted in earlier sections, the ages assigned to these events are the subject of some controversy in that some workers have suggested that the D_1–D_3 evolution was condensed into a time period at around 2500 Ma (Grew & Manton 1979, Grew *et al.* 1982, DePaolo *et al.* 1982, Sandiford & Wilson 1984), whereas others ascribe older ages of 3000–2800 Ma to D_1–D_2 (Black & James 1983, Black *et al.* 1983a, 1986a, Sheraton *et al.* 1987). Hence, documentation of older ages for D_1–D_2 in the region of highest grade metamorphism, namely the Tula and Scott mountains, is of central importance for models of the thermal history of the Napier Complex, the timescale of post-peak near-isobaric cooling (Ellis *et al.* 1980, Sheraton *et al.* 1980, Harley 1985, Harley & Black 1987), and correlations with other ultra-high temperature (UHT) granulite terrains.

Structural and textural features of the highest-grade granulites demonstrate that the high-temperature metamorphism in the Tula Mountains, Scott Mountains and Khmara Bay can be regarded as syn- and post-deformational with respect to the principal fabrics formed in D_1–D_2 in those regions. UHT metamorphic assemblages appear to be associated with both D_1 and D_2 where the fabrics can be reliably referred to either event. For example, at Mount Riiser-Larsen a sequence of sapphirine quartzites contains sapphirine-orthopyroxene-quartz layers which trace out a series of isoclinal F_1 folds with amplitudes of 5–10 m. These reflect initial growth of the highest grade minerals in D_1, though continued high-grade conditions post-dating D_1 have in this case led to recrystallization of coarser phases to polygonal granoblastic arrays of the same minerals. Unequivocal evidence of similar high grade conditions in D_2 in the Tula Mountains is seen at Mount Sones, where the highest temperature assemblages in paragneisses (sapphirine, sillimanite, quartz) define a fabric that is axial planar to tight F_2 folds in earlier gneissic layering. Similarly, at east Tonagh Island, where F_1 folds are refolded about near-co-axial F_2 closures, planar fabrics and a strong L_2 lineation are defined by the highest-temperature minerals, including sillimanite, orthopyroxene and sapphirine (Harley 1987). Post-deformational (D_1 or D_2) annealing and reaction under ultra-high temperature conditions is also indicated by the preservation of granoblastic textures in the highest-grade

https://doi.org/10.1017/S0954102097000102 Published online by Cambridge University Press

sapphirine+orthopyroxene+quartz (+osumilite) assemblages at Mount Hardy and Mount Riiser-Larsen and by the occurrence of sapphirine+quartz symplectite textures (trellis and graphic symplectites) at Dallwitz Nunatak, Tonagh Island, Mount Hardy, Crosby Nunataks and Mount Riiser-Larsen. As first proposed by Motoyoshi & Hensen (1989), such symplectites may in fact be pseudomorphs formed after lower-temperature cordierite.

The status of the D_1–M_1 event throughout the Napier Complex

The previous *c.* 3000 Ma age assignment for D_1 has relied on

1) the interpretation of the Proclamation Island orthogneiss as a syn–D_1 intrusive on the basis of its variable tectonite fabric and subparallel contact with bordering paragneisses (Black *et al.* 1986b); and

2) correlation of the fabric-forming D_1 event at Proclamation Island, here distinguished as D_1(P), with the fabric-forming event in the Tula and Scott mountains, here termed D_1(T) and D_1(S), respectively. The SHRIMP age of 2980±9 Ma derived here for the igneous crystallization of the Proclamation Island intrusion is significantly younger than the Rb–Sr whole-rock age of 3070±34 Ma (Sheraton & Black 1983) and is considered a better estimate as the latter age was derived from samples collected up to several hundreds of metres apart. The imprecise conventional multigrain U–Pb zircon age of 3030±60 Ma (Black *et al.* 1986b) is consistent with either of these dates.

The *c.* 2850 Ma Dallwitz Nunatak orthogneiss, described above and considered further below, and the 2980±9 Ma Proclamation Island charnockite cannot both be syn-deformational with respect to the same event. As a consequence there are two possibilities for the geological context of the Proclamation Island charnockite:

1) The Proclamation Island charnockite might be pre-tectonic. The structural features noted by Black *et al.* (1986b) do not exclude this possibility given that the intensity of later deformation would tend to obscure earlier discordant contacts and that key features such as an abundance of xenoliths or inclusions of paragneiss are lacking. Indeed, it is apparent from isotopic dating and detailed mapping of low strain areas in other complexly deformed terranes that orthogneisses may preserve parallelism with an apparently simple gneissic fabric, and yet be of several different, temporally discrete, generations e.g., the Canadian Shield (Percival 1990) and the Rauer Islands (Kinny *et al.* 1993). The 2980 Ma age should therefore be regarded as a maximum age for D_1(P). In this case the main tectonothermal event could be significantly younger, at *c.* 2840 Ma (see below), and D_1(P) and D_1 elsewhere would correlate. The D_1–M_1 to D_2–M_2 evolution across the entire Napier Complex would be telescoped into the short time interval between 2850–2820 Ma in this scenario.

2) The Proclamation Island charnockite might be truly syn-tectonic, whereby D_1–M_1(P) would be unrelated to that at Dallwitz Nunatak and Zircon Point, where 2850–2820 Ma ages on an orthogneiss and paragneiss respectively are correlated with the fabric-forming elements (D_1(T) and D_1(S)) and the highest-temperature granulite assemblages as described above. This would allow the possibility of two discrete "D_1" events in the Napier Complex, with the second one resulting in very high-temperature granulite metamorphism in the Tula-Scott mountain areas, but also being manifested as intrusives and reset zircons in the Napier Mountains and further north. This "two cycle/two event" model is the case shown in Fig. 10.

It should be noted that Proclamation Island is situated some 150 km north of the region of high-temperature granulites

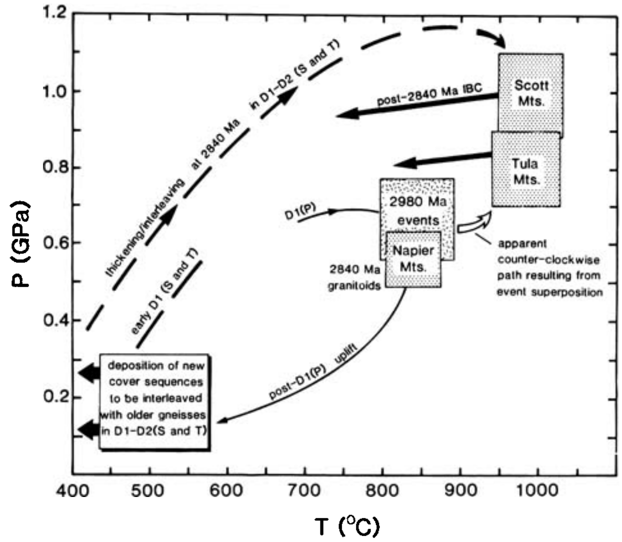

Fig. 10. Pressure-temperature diagram summarizing the polymetamorphic history envisaged for the Napier Complex between 3000–2800 Ma. The 2980 Ma intrusive and probable metamorphic events defined from Proclamation Island and associated with deformation D_1(P) are related to an early clockwise P–T loop (thin arrowed lines) and considered to have occurred over a broad region including the Napier and Tula mountains (dashed ornamented P–T box). Post D_1(P) uplift and exhumation was followed by deposition of new cover sequences, interleaved and buried in events D_1–D_2 (Scott and Tula mountains) at *c.* 2840 Ma (thick dashed and arrowed P–T paths). Stippled boxes denote *c.* 2840 Ma metamorphic conditions in sub-areas of the Napier Complex and solid arrowed lines the post-2840 Ma near isobaric cooling (Harley 1985, Harley & Black 1987). Unfilled arrow represents an apparent counter-clockwise P–T path which would be deduced for a pre-2980 Ma metasediment partially exhumed and later overprinted by higher-temperature conditions in the second event at 2840 Ma. Textures such as sapphirine+quartz after cordierite (Motoyoshi & Hensen 1989, Hensen & Motoyoshi 1992) could result from such a history.

exposed in the Tula and Scott mountains (Fig. 1). Granulites at Proclamation Island and in the Napier Mountains contain primary cordierite and biotite rather than the higher-temperature sapphirine-quartz and orthopyroxene-sillimanite assemblages characteristic of the Tula and Scott mountains and briefly described above. Hence, there is no persuasive metamorphic evidence for correlation of events on the basis of identical assemblages, and the structural case for correlation of D_1(P) with D_1(T) is neither confirmed nor required by isotopic data.

"D_2–M_2", and the significance of the c. *2840 Ma ages in the Tula and Scott mountains*

The D_2–M_2 event of Black & James (1983) has proven very difficult to date, and the age estimate has been based largely on a Rb–Sr whole-rock isochron from syn–D_2 granite at Mount Bride (2840+220/-280: Black *et al.* 1986b). Zircon populations broadly clustered at *c.* 2900 Ma, derived from a variety of localities and from both conventional multigrain (Black & James 1983) and SHRIMP zircon dating (Black *et. al.* 1986a) have also been ascribed to D_2–M_2, but the precision of this age is rather poor. This study provides three examples of relatively precisely defined U–Pb zircon ages of *c.* 2840 Ma. These are 2847±11 Ma (Proclamation Island charnockite resetting), 2850+40/-20 Ma (Dallwitz Nunatak orthogneiss) and 2822±22 Ma (Zircon Point paragneiss).

The new data for Dallwitz Nunatak in particular imply that the principal tectonothermal event in the Tula mountains region (D_1(T)) can be no older than 2850–2820 Ma, and a best-fit age for the highest grade metamorphism, consistent with all three zircon populations, is 2837±15 Ma. The Dallwitz Nunatak orthogneiss is interpreted as an example of syn-tectonic magmatism such as that observed at other localities in the Tula and Scott mountains where orthogneisses may cut paragneiss units but are then infolded with them in D_1 or D_2 structures (Mount McLennan: James & Black 1981, Khmara Bay: Sandiford & Wilson 1984). The 2822±22 Ma zircon age from the Zircon Point paragneiss may indicate that burial of sediments in the Khmara Bay area was extremely rapid and essentially contemporaneous with magmatism and ultra-high temperature metamorphism in the Amundsen Bay region, unless the high-grade event destroyed all memory of older detrital ages in this rock, an unlikely situation given the preservation of older zircon ages in the Mount Sones paragneiss.

The timescale of D_3–M_3

This tectonothermal event caused new zircon growth and/or substantial isotopic resetting of U–Pb zircon (and other dating systems) over most of the Napier Complex. A reasonably precise age estimate for D_3–M_3 of 2456+8/-5 Ma has been defined by conventional zircon dating of a syn-tectonic pegmatite in Khmara Bay (Ayatollah Island: Black *et al.* 1983b). However, zircons from a pegmatite at McIntyre Island yielded an older mean $^{207}Pb/^{206}Pb$ age of 2474±3 Ma for D_3 (Black *et al.* 1983b), which was supported by a SHRIMP age of 2479±23 Ma from reset zircons in the Mount Sones orthogneiss (Black *et al.* 1986a). Maximum age limits on D_3–M_3 are 2474+6/-3 Ma (James & Black 1981) for a pre-D_3 leuconorite at Mount Hardy in the Tula mountains and 2481±3 Ma for pre-D_3 granite further northwards at Simmers Peak (Black *et al.* 1986b) in the Napier Mountains.

Two of the newly analysed rocks, the Dallwitz Nunatak orthogneiss and the Zircon Point paragneiss, contain some zircons which crystallized at 2481±4 Ma and 2508±38 Ma, confirming that D_3–M_3 occurred as early as 2480 Ma. However, the concordance of the data for the younger (2456+8/-5 Ma) Khmara Bay pegmatite age makes it unlikely that it is erroneous. Therefore, zircon growth and resetting occurred at different times during a relatively protracted D_3–M_3 event (25 Ma duration), perhaps promoted by fluid ingress rather than solely by increased temperatures.

New results on the age of metamorphism in the Napier Complex have been presented by Owada *et al.* (1995) and Osanai *et al.* (1995), who obtained Sm–Nd data on felsic and mafic orthogneisses and a suite of paragneisses from Tonagh Island. A Sm–Nd isochron based upon 10 samples of quartz-orthopyroxene gneiss, orthopyroxene-garnet gneiss and orthopyroxene-clinopyroxene-garnet gneiss gives an age of 2479±137 Ma and an initial Nd ratio (0.508960) that would translate to a highly negative εNd(T) (Osanai *et al.* 1995). Four felsic gneisses sampled from within 40 m of each other gave an isochron age of 2489±47 Ma with εNd(T) of -9.0, also suggesting a long-lived crustal residency prior to 2500 Ma (Owada *et al.* 1995). The *c.* 2480 Ma ages defined by these studies have been ascribed to UHT metamorphism and anatexis at Tonagh Island (i.e. the D_1–M_1 or D_2–M_2 events), but are in coincident with the zircon ages ascribed to D_3–M_3 in our present chronology.

Conclusions and a revised chronology

The new isotopic results and the interpretation presented here are summarized in Table I, where they can be compared with the previous chronology developed by several groups and summarized in Sheraton *et al.* (1987). SHRIMP U–Pb zircon data indicate that, although it is one of the most ancient of preserved terrestrial terranes, the Napier Complex is probably not as old as previously reported from Pb–Pb whole rock and ion-microprobe studies. Although the 3840–3770 Ma orthogneisses may have yielded detritus for some sediments in the Tula Mountains area, they appear to be only a minor component of the presently sampled crust.

A key difference between the new chronology and the previous, generally accepted, chronology for the Napier Complex is recognition that the UHT metamorphic event in the Napier Complex is *no older* than *c.* 2840 Ma. From the evidence of the Zircon Point paragneiss we also suggest that a rapid sequence of sedimentation, crustal thickening and magmatism took place in Enderby Land between 2850 Ma and 2820 Ma, involving the burial and granulite-facies metamorphism of sediments deposited only recently beforehand, as well as an older basement containing granitoids and metasediments (Fig. 10). These principal tectonothermal events in the Tula Mountains, Scott Mountains and Khmara Bay are significantly younger than the age previously ascribed to D_1 based on the Proclamation Island charnockite, now reliably dated at 2980±9 Ma. The Proclamation Island charnockite may simply date an early magmatic episode or the age of a significant tectonothermal event, (D_1P), unrelated to the later UHT metamorphism recorded further southwest.

The previous concept of a single D_1–M_1 event which occurred under different granulite P–T conditions across the Napier Complex at *c.* 3000 Ma (e.g. Sheraton *et al.* 1987, Harley & Black 1987, Harley & Hensen 1990) is highly improbable in the light of these new data. We propose that two discrete and unrelated "D_1" events may have occurred, with the second one [D_1(T) and D_1(S)] responsible for UHT granulite metamorphism in the Tula-Scott mountains areas, and manifesting itself as 2840 Ma intrusive rocks and reset zircons (Black *et al.* 1986b) in the Napier Mountains and areas farther north (Fig. 10). In this two-event model the first event, represented by D_1(P), could have produced cordierite-bearing mineral assemblages in appropriate rock types in the northern part of the Napier Complex, and perhaps in the Tula and Scott mountains as well. These early metamorphic rocks were later interleaved with new (post-2980 Ma) sediments deposited up to *c.* 2840 Ma and upgraded to sapphirine-quartz assemblages during the second event, D_1–D_2 (T or S). In this model partial exhumation of the crust in the Napier Complex occurred in the 150 million years between the two major events. Near isobaric cooling (IBC) ensued only after *c.* 2840 Ma until at least 2480–2450 Ma (the age of D_3–M_3), and perhaps even through to 1000 Ma (Harley 1985).

The polymetamorphic character of some paragneisses in this model offers an alternative explanation of the replacement of cordierite by symplectitic sapphirine + quartz, an important texture described and interpreted in terms of a continuous counter-clockwise P–T evolution by Motoyoshi & Hensen (1989), who also suggested a two-event evolution to explain textural features in osumilite-bearing rocks (Hensen & Motoyoshi 1992). In the revised model presented here (Fig. 10) the cordierite may have been produced in the first metamorphic event (M1) associated with D_1(P) at 2980 Ma, and the sapphirine and quartz in the unrelated UHT metamorphism (M2) superimposed at 2850–2820 Ma.

A corollary of this "two-event" model is that the north–south grade variation seen in the Napier Complex, and part of the north–south apparent gradient in peak pressure (Harley & Hensen 1990, fig. 1), might be artefacts of the superposition of the two separate events, one at 0.5–0.8 GPa and750–850°C occuring across the whole complex, and the second one upgrading and "up-pressuring" the earlier rocks in the Amundsen Bay area. Metamorphism of a post-2980 Ma cover sequence at 2850–2820 Ma would give the mineral assemblage and isobar distribution deduced for the southwest part of the Napier Complex (Fig. 1), and an apparent "counter-clockwise" P–T history could be produced in the older paragneises compared with a clockwise or simple heating path in the interleaved cover. This model predicts that the age of the main metamorphism and the minimum depositional ages for sediments in the Napier Mountains and areas further north should be older than in the UHT metamorphic region, and that only the older paragneisses in the Amundsen Bay area will preserve sapphirine + quartz pseudomorphs after cordierite. These key predictions are testable, and will provide a focus for further isotopic studies of this remarkable ultra-high temperature Archaean metamorphic terrain.

Acknowledgements

Chris Foudoulis, Lance Keast, Brad McDonald and Mick Bower are thanked for their technical support. The manuscript was constructively reviewed by John Sheraton and Bob Tingey. Further reviews by Ed Grew, Alastair Moyes and Bob Pankhurst are appreciated. Logistic support in the field was provided by the Antarctic Division, Department of the Arts, Sport, the Environment, Tourism and Territories. The contribution of L.P. Black is published with the permission of the Executive Director, Australian Geological Survey Organisation.

References

Black, L.P. & James, P.R. 1983. Geological history of the Archaean Napier Complex in Enderby Land. *In* Oliver, R.L., James, P.R. & Jago, J.B., *eds. Antarctic earth science.* Canberra: Australian Academy of Science and Cambridge: Cambridge University Press, 11-15.

Black, L.P. & McCulloch, M.T. 1987. Evidence for isotopic equilibration of Sm–Nd whole-rock systems in early Archaean crust of Enderby Land, Antarctica. *Earth and Planetary Science Letters*, **82**, 15-24.

Black, L.P., James, P.R. & Harley, S.L. 1983a. The geochronology, structure and metamorphism of early Archaean rocks at Fyfe Hills, Enderby Land, Antarctica. *Precambrian Research*, **21**, 197-222.

Black, L.P., James, P.R. & Harley, S.L. 1983b. Geochronology and geological evolution of metamorphic rocks in the Field Islands area, East Antarctica. *Journal of Metamorphic Geology*, **1**, 277-303.

Black, L.P., Williams, I.S. & Compston, W. 1986a. Four zircon ages from one rock: the history of a 3930 Ma-old granulite from Mount Sones, Antarctica. *Contributions to Mineralogy and Petrology*, **94**, 427-437.

Black, L.P., Sheraton, J.W. & James, P.R. 1986b. Late Archaean granites of the Napier Complex, Enderby Land, Antarctica: A comparison of Rb–Sr, Sm–Nd and U–Pb isotopic systematics in a complex terrain. *Precambrian Research*, **32**, 343-368.

Black, L.P., Harley, S.L., Sun, S.-S. & McCulloch, M.T. 1987. The Rayner Complex of East Antarctica: complex isotopic systematics within a Proterozoic mobile belt. *Journal of Metamorphic Geology*, **5**, 1-26.

Black, L.P., Sheraton, J.W. & Kinny, P.D. 1992. Archaean events in Antarctica. *In* Yoshida, Y. *et al., eds. Recent progress in Antarctic* *earth science*. Tokyo: TERRAPUB, 1-6.

Compston, W. & Williams, I.S. 1982. Protolith ages from inherited zircon cores measured by a high mass-resolution ion microprobe (Abstract). *Fifth international symposium on geochronology, cosmochronology and isotope geology, Nikko, Japan, June 27–July 2*, 63-64.

Compston, W., Williams, I.S. & Meyer, C. 1984. U–Pb geochronology of zircons from Lunar breccia 73217 using a sensitive high mass-resolution ion microprobe. *In Proceedings of the Fourteenth Lunar and Planetary Science Conference. Journal of Geophysical Research*, **89** (Supplement), B525-534.

Compston, W., Kinny, P.D., Williams, I.S. & Foster, J.J. 1986. The age and lead loss behaviour of zircons from the Isua Supracrustal Belt as determined by ion microprobe. *Earth and Planetary Science Letters*, **80**, 71-81.

Cumming, G.L. & Richards, J.R. 1975. Ore lead isotope ratios in a continuously changing Earth. *Earth and Planetary Science Letters*, **28**, 155-171.

Dallwitz, W.B. 1968. Co-existing sapphirine and quartz in granulite from Enderby Land, Antarctica. *Nature*, **219**, 476-477.

DePaolo, D.J., Manton, W.I., Grew, E.S. & Halpern, M. 1982. Sm–Nd, Rb–Sr and U–Th–Pb systematics of granulite facies rocks from Fyfe Hills, Enderby Land, Antarctica. *Nature*, **298**, 614-618.

Ellis, D.J. 1980. Osumilite-sapphirine-quartz granulites from Enderby Land, Antarctica: P–T conditions of metamorphism, implications for garnet-cordierite equilibria and the evolution of the deep crust. *Contributions to Mineralogy and Petrology*, **74**, 201-10.

Ellis, D.J. 1983. The Napier and Rayner Complexes of Enderby Land, Antarctica: contrasting styles of metamorphism and tectonism. *In* Oliver, R.L., James, P.R. & Jago, J.B., *eds. Antarctic earth science*. Canberra: Australian Academy of Science and Cambridge: Cambridge University Press, 20-24.

Ellis, D.J., Sheraton, J.W., England, R.N. & Dallwitz, W.B. 1980. Osumilite-sapphirine-quartz granulites from Enderby Land, Antarctica – mineral assemblages and reactions. *Contributions to Mineralogy and Petrology*, **72**, 123-43.

Froude, D.O., Ireland, T.R., Kinny, P.D., Williams, I.S., Compston, W., Williams, I.R. & Myers, J.S. 1983. Ion microprobe identification of 4100–4200 m.y. old terrestrial zircons. *Nature*, **304**, 616-619.

Grew, E.S. 1980. Sapphirine + quartz association from Archaean rocks in Enderby Land, Antarctica. *American Mineralogist*, **65**, 821-836.

Grew, E.S. & Manton, W.I. 1979. Archean rocks in Antarctica: 2.5 billion-year uranium-lead ages of pegmatites in Enderby Land. *Science*, **206**, 443-445.

Grew, E.S., Manton, W.I. & Sandiford, M.A. 1982. Geochronologic studies in East Antarctica: age of pegmatites in Casey Bay, Enderby Land. *Antarctic Journal of the United States*, **17**(5), 1-2.

Harley, S.L. 1983. Regional geobarometry-geothermometry and metamorphic evolution of Enderby Land, Antarctica. *In* Oliver, R.L., James, P.R. & Jago, J.B., *eds. Antarctic earth science*. Canberra: Australian Academy of Science and Cambridge: Cambridge University Press, 25-30.

Harley, S.L. 1985. Garnet-orthopyroxene bearing granulites from Enderby Land, Antarctica: metamorphic pressure-temperature-time evolution of the Archaean Napier Complex. *Journal of Petrology*, **26**, 819-856.

Harley, S.L. 1987. Pyroxene-bearing granulites from Tonagh Island, Enderby Land, Antarctica: Further evidence for very high temperature (>950°C) archaean regional metamorphism in the Napier Complex. *Journal of Metamorphic Geology*, **5**, 341-356.

Harley, S.L. & Black, L.P. 1987. The Archaean geological evolution of Enderby Land, Antarctica. *In* Park, R.G. & Tarney, J., *eds. Evolution of the Lewisian and comparable Precambrian high grade terrains*. Geological Society Special Publication No. 27, 285-296.

Harley, S.L. & Hensen, B.J. 1990. Archaean and Proterozoic high-grade terranes of East Antarctica (40°E–60°E): A case study of the diversity in granulite facies metamorphism. *In* Ashworth, J.R. & Brown, M., *eds. High temperature metamorphism and crustal anatexis*. London: Unwin Hyman, 320-370.

Hensen, B.J. & Motoyoshi, Y. 1992. Osumilite-producing reactions in high-temperature granulites from the Napier Complex, East Antarctica: tectonic implications. *In* Yoshida, Y., Kaminuma, K. & Shiraishi, K., *eds. Recent progress in Antarctic earth science*. Tokyo: TERRAPUB, 87-92.

James, P.R. & Black, L.P. 1981. A review of the structural evolution and geochronology of the Archaean Napier Complex of Enderby Land, Australian Antarctic Territory. *In* Glover, J.E & Groves, D.I., *eds.* Archaean geology. Geological Society of Australia Special Publications, No. 7, 71-83.

Kinny, P.D. 1986. 3830 Ma zircons from a tonalitic Amitsoq Gneiss in the Godthab district of southern west Greenland. *Earth and Planetary Science Letters*, **79**, 337-347.

Kinny, P.D., Black, L.P. & Sheraton, J.W. 1993. Zircon ages and the distribution of Archaean and Proterozoic rocks in the Rauer Islands. *Antarctic Science*, **5**, 193-206.

Krylov, A.Ya. 1972. Antarctic geochronology. *In* Adie, R.J., *ed. Antarctic geology*. Oslo: Universitetsforlaget, 491-494.

Liu, D.Y., Nutman, A.P., Compston, W., Wu, J.S. & Shen, Q.H. 1992. Remnants of 3800 Ma crust in the Chinese part of the Sino-Korean Craton. *Geology*, **20**, 339-342.

Lovering, J.F. 1979. The evidence for ~4000 m.y. crustal material in Archaean times (Abstract). *Journal of the Geological Society of Australia*, **26**, 268.

Lovering, J.F. 1980. Proto-crustal Nuclei: Ion-microprobe evidence for *c.* 4000 Ma crustal material in Archaean terrains in West Greenland and Enderby Land (Antarctica)?(Abstract)*In* Glover, J.E. & Groves, D.I., *eds. Archaean geology*. Geological Society of Australia Special Publications No. 7, 84-85.

Motoyoshi, Y. & Hensen, B.J. 1989. Sapphirine-quartz-orthopyroxene symplectites after cordierite in the Archaean Napier Complex, Antarctica: evidence for a counter-clockwise P–T path. *European Journal of Mineralogy*, **1**, 467-471.

Nutman, A.P., Friend, C.R.L., Kinny, P.D. & McGregor, V.R. 1993. Anatomy of an Early Archaean gneiss complex: 3900–3600 Ma crustal evolution in southern Greenland. *Geology*, **21**, 415-418.

Osanai, Y., Owada, M., Shiraishi, K., Hensen, B.J. & Tsuchiya, N. 1995. Metamorphic evolution of deep crustal high temperature granulites from Tonagh Island in the Archaean Napier Complex, East Antarctica. (Abstract) *Proceedings Seventh International Symposium on Antarctic Earth Sciences, Siena*, 289.

Owada, M., Osanai, Y., Kagami, H & Shiraishi, K. 1995. Isotopic equilibration of early to middle Archaean crust by late Archaean tectonothermal events in the Napier Complex, East Antarctica. (Abstract) *Proceedings Seventh International Symposium on Antarctic Earth Sciences, Siena*, 292.

Percival, J.A. 1990. Archean tectonic setting of granulite terranes of the Superior Province, Canada: a view from the bottom. *In* Vielzeuf, D. & Vidal, P., *eds. Granulites and crustal evolution*. Dordrecht: Kluwer, 171-193.

Ravich, M.G. & Kamenev, Ye.N. 1975. *Crystalline basement of the Antarctic Platform*. New York: John Wiley.

Ravich, M.G., Sobotovich, E.V., Kamenev, Ye.N. & Rudnik, V.A. 1975. Late Azoic age of the oldest rocks of Antarctica. *Doklady Akademii Nauk SSSR*, **216**, 115-117.

Sandiford, M.A. & Wilson, C.J.L. 1984. The structural evolution of the Fyfe Hills – Khmara Bay region, Enderby Land, East Antarctica. *Australian Journal of Earth Sciences*, **31**, 403-426.

Schiotte, L., Compston, W. & Bridgwater, D. 1989. Ion probe U–Th–Pb dating of polymetamorphic orthogneiss from Northern Labrador, Canada. *Canadian Journal of Earth Sciences*, **26**, 1533-1556.

Sheraton, J.W. & Black, L.P. 1983. Geochemistry of Precambrian gneisses: relevance for the evolution of the East Antarctic Shield.

Lithos, **16**, 273-296.

SHERATON, J.W., OFFE, L.A., TINGEY, R.J. & ELLIS, D.J. 1980. Enderby Land, Antarctica – an unusual Precambrian high-grade metamorphic terrain. *Journal of the Geological Society of Australia*, **27**, 1-18.

SHERATON, J.W., TINGEY, R.J., BLACK, L.P., OFFE, L.A. & ELLIS, D.J. 1987. Geology of Enderby Land and western Kemp Land, Antarctica. *Bureau of Mineral Resources, Australia, Bulletin*, No. 223, 51 pp.

SOBOTOVICH, E.V., KAMENEV, YE.N., KOMARISTYY, A.A. & RUDNIK, V.A. 1976. The oldest rocks of Antarctica (Enderby Land). *International Geology Review*, **18**, 371-388.

WIEDENBECK, M. 1995. An example of reverse discordance during ion microprobe zircon dating: an artifact of enhanced ion yields from a radiogenic labile Pb. *Chemical Geology*, **125**, 197-218.

WILLIAMS, I.S., COMPSTON, W., BLACK, L.P., IRELAND, T.R. & FOSTER, J.J. 1984. Unsupported radiogenic Pb in zircon: a cause of anomalously high Pb–Pb, U–Pb and Th–Pb ages. *Contributions to Mineralogy and Petrology*, **88**, 322-327.

Appendix: Sample Descriptions

78285007 Mount Sones. Granodioritic-tonalitic composition orthogneiss composed of anti-perthitic plagioclase, quartz, orthopyroxene, and accessory opaque minerals, apatite, zircon and monazite. Zircons have a wide range of morphologies. Most zircons are brown, subhedral, elongated and strongly zoned; weakly zoned and optically homogeneous phases are also present; cores are common. Many brown zircons (average grain size is *c.* 300 x 200 mm) are mantled by recrystallized clearer zircon. Pale pink, optically homogeneous and relatively equant zircons are *c.* 100 mm in diameter.

77283465 Mount Sones. Tonalitic orthogneiss composed of antiperthite, quartz, orthopyroxene, 6% garnet and opaque minerals. Garnet is largely confined to a discrete layer. Zircons are brown and elongate (300 x 150 mm) and often contain distinct elongated cores. Most grain terminations are rounded but some are sharp and euhedral. Some grains are noticeably zoned; others are relatively homogeneous.

78285013 Gage Ridge. Massive granitic gneiss composed of mesoperthite, quartz, 0.5% orthoproxene and accessory zircon. Zircons are medium to dark brown and well rounded. Although some grains are relatively equant (200 mm in diameter), most are elongated (450x150 mm). Distinct "pinching" of some grains may reflect metamorphic recrystallization. Cores are common. Many are elongated and zoned, but relatively equant, unzoned cores are also present.

80285045 Proclamation Island. Charnockite composed of perthite, quartz, plagioclase, orthopyroxene, hornblende and accessory opaque minerals, clinopyroxene, apatite and zircon. Zircons are euhedral to subhedral, relatively coarse and elongated (average 450 x 200 mm, but ranging up to 600 mm in length). Some grains are strongly zoned but traces of fine-scale zoning is most common and unzoned grains are also present. Silicate and fluid inclusions are relatively common. Zircon grain terminations are rarely sharp and euhedral (secondary pyramids); most are well rounded. Distinctly "pinched" grains also occur, reflecting metamorphic modification.

78285005 Dallwitz Nunatak. Granitic (charnockitic) gneiss composed of mesoperthite, quartz and orthopyroxene. Accessory zircon is brown and mostly elongated (averaging *c.* 450 x 150 mm). Although now somewhat rounded, most grains preserve vestiges of their original igneous terminations. Equant grains are also present. Both varieties of zircon have distinct large cores (usually zoned) surrounded by strongly zoned rims. Annealing/recrystallization has led to the differential removal of sharp zonation in some grains.

77283267 Mount Sones: Paragneiss composed of antiperthite, quartz and garnet. Zircons are dominated by elongated (averaging *c.* 250 x 100 mm) and dark brown grains. These well-rounded grains are mostly strongly zoned, commonly contain cores, and are markedly cracked. Also present are paler, rounded, equant (~100 mm diameter) grains of probable metamorphic origin.

80285037 Zircon Point, Khmara Bay. Paragneiss composed of porphyroblastic garnet and highly strained mesoperthite and quartz, in a quartzofeldspathic matrix. Minor secondary muscovite and biotite are present, especially near garnet. Zircon grains are highly rounded and generally pale brown. Most zircons have diameters of *c.* 200 mm, and are relatively equant. Less common elongate grains, some of which are "pinched" at mid-length, average *c.* 350 x 200 mm. Most grains are faintly zoned or unzoned (low U and Th). However, euhedral zoning is pronounced in some grains and indicates that a substantial portion of both grain types are originally of igneous origin, even though they have been strongly modified. Rounded, relatively equant, anhedral cores are common.